



**REPUBLIC OF TURKEY
YILDIZ TECHNICAL UNIVERSITY
FACULTY OF ELECTRICAL-ELECTRONICS ENGINEERING
DEPARTMENT OF CONTROL AND AUTOMATION ENGINEERING**

GRADUATION PROJECT

**DESIGN, SIMULATION AND EVALUATION OF ADAPTIVE
CRUISE CONTROL FOR VEHICLES**

Advisor: Asst. Prof. Dr. Mumin Tolga EMİRLER

19016909 – Mustafa TURSUN

20015609- Anıl YILMAZŞAMLI

Istanbul, 2024

T.C.
YILDIZ TECHNICAL UNIVERSITY
DEPARTMENT OF CONTROL AND AUTOMATION ENGINEERING
DESIGN, SIMULATION AND EVALUATION OF ADAPTIVE CRUISE CONTROL
FOR VEHICLES

A graduation project submitted by Mustafa TURSUN and Anıl YILMAZŞAMLI in partial fulfillment of the requirements for the degree of bachelor is approved by the committee on 31.05.2024 in Department of Control and Automation Engineering, Faculty of Electrical and Electronics Engineering.

Examining Committee

Asst. Prof. Dr. Mumin Tolga EMİRLER

Yıldız Technical University

Yıldız Technical University

Yıldız Technical University

I hereby declare that I have obtained the required legal permissions during data collection and exploitation procedures, that I have made the in-text citations and cited the references properly, that I haven't falsified and/or fabricated research data and results of the study and that I have abided by the principles of the scientific research and ethics during my graduation project under the title of Design, Simulation and Evaluation of Adaptive Cruise Control for Vehicles supervised by my advisor, Asst. Prof. Dr. Mumin Tolga EMİRLER. In the case of a discovery of false statement, I am to acknowledge any legal consequence.

Mustafa TURSUN

İmza



Anıl YILMAZŞAMLI

İmza



ABSTRACT

In this graduation thesis, automatic transmission vehicle modeling and Adaptive Cruise System design were made. The purpose of writing the thesis is to understand how vehicles are modeled and to design a controller for a nonlinear system. Design were made the different components of the vehicle and the driver character. The controller design was made with different approaches applied. For these methods, modern methods and the genetic algorithm method, which is a computer-based machine learning optimization method, have been applied. While designing the controller for the system, MATLAB functions such as SISO Tool, Global Optimization Tool, System Identification and Control Design Tool were used.

In the thesis, the way of the methods, MATLAB codes of the functions and graphical results are explained with detailed proofs.

June, 2024

Mustafa TURSUN and Anıl YILMAZŞAMLI

ÖNSÖZ

Bu bitirme tezinin hazırlanma sürecinde bilgi ve tecrübesiyle yönlendiren, çalışma boyunca anlayışla yaklaşan saygıdeğer danışmanımız Dr.Öğr.Üyesi Mumin Tolga EMİRLER'e, eğitim-öğrenim hayatımıza desteklerini esirgemeyen ailemize teşekkürü borç biliriz. Son olarak bizleri yönlendiren ve destek veren Kontrol ve Otomasyon Mühendisliği akademisyenlerimize ve arkadaşımız Eyüp OKUMUŞ'a katkılarından dolayı teşekkür ederiz.

Haziran, 2024

Mustafa TURSUN ve Anıl YILMAZŞAMLI

CONTENT

ABSTRACT.....	iv
ÖNSÖZ.....	v
CONTENT.....	1
LIST OF SYMBOLS	3
LIST OF ABBREVIATIONS	7
LIST OF FIGURES.....	8
LIST OF TABLES.....	10
ABSTRACT.....	11
ÖZET	12
SECTION 1	13
1. INTRODUCTION.....	13
1.1 Literature Survey	13
1.2 Objective of Study	13
SECTION 2	19
2. PRELIMINARIES	19
2.1 Cruise Systems for Vehicles	19
2.1.1 Cruise Control System.....	19
2.1.2 Adaptive Cruise Control for Vehicles	19
2.1.3 Driving Enhancement.....	21
2.1.4 General Informations of Cruise Control Systems	21
2.2 Control Problem of the ACC for Vehicles	24
2.2.1 Distance Control of Two Vehicles	24
2.3 Genetic Algorithm	25
2.4 Hardwares for ACC	28
SECTION 3	30
3. MATHEMATICAL MODELING OF THE VEHICLE	30
3.1 Linear Modeling for Longitudinal Dynamics	30
3.1.1 Aerodynamic Drag Force	30

3.1.2	Longitudinal Tire Force	31
3.1.3	Rolling Resistance	31
3.1.4	Upper Level Controller.....	32
3.2	Nonlinear Modeling for Longitudinal Dynamics	33
3.2.1	Lower Level Controller	34
3.3	Safe Distance Control	44
SECTION 4	46
4. ADAPTIVE CRUISE CONTROL MODELING.....		46
4.1	Estimation of Transfer Function	46
4.1.1	System Identification Toolbox	47
4.2	Feedback Controller Design	50
4.3	Adaptive Cruise Controller Design	52
4.3.1	ACC Controller Design with PD Controller	54
4.3.2	ACC Controller Tuning with Genetic Algorithm	63
4.4	Comparison of the Designed PD Controller and GA Tuned Controller	77
SECTION 5	80
5. REALISTIC LIMITS, CONDITIONS AND CONSTRAINS TAKEN INTO CONSIDERATION IN THE DESIGN OF THE PROJECT		80
SECTION 6	81
6. CONCLUSION.....		81
REFERENCES.....		83
RESUME.....		85

LIST OF SYMBOLS

N_{in}	Speed of turbine (torque converter output) transmission input speed
T_{in}, T_{out}	Transmission input and output torques
N_{in}, N_{out}	Transmission input and output speed (RPM)
I_v	Vehicle inertia
N_w	Wheel speed (RPM)
R_{fd}	Final drive ratio
R_{load0}, R_{load2}	Friction and aerodynamics drag coefficients
T_{load}, T_{brake}	Load and brake torques
mph	Vehicle linear velocity
R_{TR}	$f_4(gear)$ =transmission ratio
F_{xf}	Longitudinal tire force at the front tires
F_{xr}	Longitudinal tire force at the rear tires
F_{aero}	Equivalent longitudinal aerodynamic drag force
R_{xf}	Force due to rolling resistance at the front tires
R_{xr}	Force due to rolling resistance at the rear tires
m	Mass of the vehicle
g	Acceleration due to gravity
θ	Angle of inclination of the road on which the vehicle is traveling
ρ	Mass density of air

C_d	Aerodynamic drag coefficient
A_F	Frontal area of the vehicle
V_x	Longitudinal vehicle velocity
V_{wind}	Wind velocity
F_{zf}	Normal force of front tires
F_{zr}	Normal force of rear tires
h_{aero}	Height of the location at which the equivalent aerodynamic force acts
ℓ_f	Longitudinal distance of the front axle from the c.g. of the vehicle
ℓ_r	Longitudinal distance of the rear axle from the c.g. of the vehicle
I_{ei}	Moment of inertia of the engine and the impeller
N_e	Engine speed(rpm)
T_e, T_i	Engine and impeller tork
V_{eff}	Effective linear velocity of rotating tire
β	Parameter related to aerodynamic drag coefficient calculation
σ_x	Slip ratio
ω_e	Rotational engine speed
ω_t	Angular speed of turbine on torque converter
T_p	Pump torque

T_t	Turbine torque
T_{wheels}	Torque transmitted to the wheels
ω_w	Angular speed of wheel
τ	Time constant in gear change dynamics
R	Gear ratio
ω_{wf}, ω_{wr}	Angular speed of front and rear wheels respectively
h	Height of c.g. of vehicle
$d_{r,i}$	Desired distance between car i and its predecessor
d_i	Actual distance between car i and its predecessor
e_i	Distance error of car i
$e_{n,i}$	Error state n of car i
h	Time headway (used to calculate speed-dependent distance)
L_i	Car length
s_i	Absolute position of car i
v_i	Absolute speed of car i
t_{ts}	Tracking Time
r_i	Standstill distance between car i and its predecessor
ζ	Damping ratio
w_n	Natural frequency

Q	State weighting matrix
T_s	Settling time
R	Control input weighting matrix
J	Cost function of LQR
x_{ego}	Position of the ego vehicle
x_{lead}	Position of the lead vehicle
K_C	Gain constant of ideal derivative compensator
θ_i	The angles of the zeros and poles of the open loop transfer function to the desired pole
θ_D	Angle of the zero coming from the ideal derivative compensator to the desired pole
z_d	The location of the zero of the ideal derivative compensator at the root locus

LIST OF ABBREVIATIONS

ACC	Adaptive Cruise Control
CC	Cruise Control
GA	Genetic Algorithm
LIDAR	Light Detection and Ranging
RADAR	Radio Detection and Ranging
ECU	Electronic Control Unit
OL	Open Loop
CL	Close Loop
OLTF	Open Loop Transfer Function
LQR	Linear Quadratic Regulator
PID	Proportional Integral Derivative
PD	Proportional Derivative
PI	Proportional Integral

LIST OF FIGURES

	Page
Figure 1.1: A fatigue-risk graph for long tour drivers [4].....	15
Figure 2.1: Waymo full-autonomous taxi [20].....	20
Figure 2.2: Representation of cruise control button.	22
Figure 2.3: Working principle of the ACC [7]	23
Figure 2.4: Distance representation between the vehicles [19]	24
Figure 2.5: Representation of an individual (parameter) in genetic algorithms. This binary representation encodes two parameters that are each represented with a 3-bit binary expression. Each parameter value has an associated cost (right), with red indicating the lowest cost solution [2]	26
Figure 2.6: Genetic operations to advance one generation of parameters to the next in a genetic algorithm [2].....	27
Figure 2.7: Doppler effect [9].....	29
Figure 3.1: Longitudinal forces applied moving car on a inclined road [1].	30
Figure 3.2: Dynamic representation of the vehicle in inclined road [1]	32
Figure 3.3: The Upper Level Controller Scheme	33
Figure 3.4: Vehicle System Block Structure [11].....	33
Figure 3.5: Power flow and loads in vehicle drivetrain [1]	34
Figure 3.6: This block model shows the outputs from the powertrain and engine according to the throttle pedal angle.	34
Figure 3.7: Simulink model of the Auto Transmission vehicle and include driver characteristic for control the throttle.....	35
Figure 3.8: Inside of the engine model for vehicle and look-up table for engine torque characteristic map.	36
Figure 3.9: Block representation of engine inertia model [1]	36
Figure 3.10: Block representation of transmission model [1]	37
Figure 3.11: Inside of the transmission block for auto transmission vehicle and also include torque converter.	38
Figure 3.12: Subsystem of the torque converter.....	39
Figure 3.13: Subsystem of the TransmissionRatio block. The look-up table for gears and gear ratio for 4-gear forward vehicle.	39
Figure 3.14: Subsystem of the vehicle block.	41
Figure 3.15: Relation between speed-throttle and shifting points [12]	42
Figure 3.16: 4-gear vehicle shifting algorithm in Simulink	42
Figure 3.17 Block representation of wheel inertia dynamic	43
Figure 3.18: Throttle Brake Subsystem.....	44
Figure 4.1: Open-Loop system representation with acceleration input.	46
Figure 4.2: Output of the Nonlinear Vehicle in order Throttle Pressure, Engine Torque and Velocity. This response get from constant 100 kmph as input.	48
Figure 4.3: System Identification of Nonlinear Vehicle	48
Figure 4.4: Estimated Results for Nonlinear Vehicle	49
Figure 4.5: Estimated Transfer Function of Nonlinear Vehicle.....	50
Figure 4.6: Close-loop Feedback Controller. In this figure, $C(s)$ is representing as a controller and $G(s)$ is plant of the vehicle. By sensors measure $H(s)$ as a feedback.	51

Figure 4.7: All of the Vehicle block diagram in MATLAB/Simulink.	53
Figure 4.8: ACC basic block diagram structure.	53
Figure 4.9: All of the ACC vehicle block diagram in MATLAB/Simulink.	53
Figure 4.10: Simplified Block Diagram of the ACC Model.....	54
Figure 4.11: Root Locus of the System According to Specified Criteria [15].....	56
Figure 4.12: Diagram showing angle measurements from open loop poles and open loop zero to desired closed loop pole	56
Figure 4.13: Root Locus of the Closed-Loop of the Compensated System	58
Figure 4.14: Step response of the uncompensated system displayed with the Matlab Sisotool Command [15]	58
Figure 4.15: Step response of the compensated system displayed with the Matlab Sisotool Command [15].....	59
Figure 4.16: Velocity Comparision of Lead Vehicle and PD Controlled Ego Vehicle	60
Figure 4.17: Comparison of the taken distance of the lead vehicle and PD controlled ego vehicle	61
Figure 4.18: The output signal of the PD controller designed using the root locus technique.	62
Figure 4.19: Distance Between Lead Vehicle and Ego Vehicle by the PD Controlled Scenario	63
Figure 4.20: Code for the define the ACC system and Genetic algorithm function [17]	66
Figure 4.21: Code for pidtest function for estimate PID parameters as P for parms (1), I for parms (2) and D for parms (3) [17]	66
Figure 4.22: Velocity input of the vehicle in lead.	68
Figure 4.23: Velocity output of the lead vehicle.....	69
Figure 4.24: Distance taken of the lead vehicle.....	69
Figure 4.25: Genetic warmth map output of the genetic algorithm and relation with cost function J by the scenario 1.	70
Figure 4.26: Genetic warmth map output of the genetic algorithm and relation with cost function J by the scenario 2.	71
Figure 4.27: Genetic warmth map output of the genetic algorithm and relation with cost function J by the scenario 3.	71
Figure 4.28: Genetic warmth map output of the genetic algorithm and relation with cost function J by the scenario 4.	72
Figure 4.29: Genetic warmth map output of the genetic algorithm and relation with cost function J by the scenario 5.	72
Figure 4.30: Comparison of the output signals PID tuned with genetic algorithm.	73
Figure 4.31: Covered distance of the vehicles by the scenearios of the Genetic Algorithm estimated PID tuning.	74
Figure 4.32: Distance difference between the lead and ego vehicles.....	74
Figure 4.33: Velocity comparison of the vehicles by the scenarios.....	75
Figure 4.34: Step response of the scenario 4.	76
Figure 4.35: Step response of the scenario 5	76
Figure 4.36: Comparison of the Designed PD Controller and GA Tuned Controller	77
Figure 4.37: Vehicles Distance Comparison of the Two Different Controller	78
Figure 4.38: Control Signal Comparison of the PD Controller and GA Tuned Controller	78
Figure 4.39: Distance Between Lead Vehicle and Ego Vehicle's Controllers.....	79

LIST OF TABLES

	Page
Table 1.1: Simulation results summary table: indicates the fuel economy benefits of vehicles with ACC compared to the driver [5]	16
Table 1.2: The table showing the number of fatal and injury accidents by years [6]	17
Table 3.1: Transmission gear rates.	40
Table 4.1: Scenarios for tuning PID parameters	67
Table 4.2: Tuned PID values and cost (J) values according to different scenarios.....	70

**DESIGN, SIMULATION AND EVALUATION OF ADAPTIVE CRUISE CONTROL
FOR A VEHICLES**

Mustafa TURSUN and Anil YILMAZŞAMLI

Department of Control and Automation Engineering

Graduation Project

Advisor: Asst. Prof. Dr. Mumin Tolga EMİRLER

In this graduation thesis, cruise systems technologies are mentioned. The current application of cruise systems is explained. It is possible to further develop the system with different communication methods, but traditional sensors are discussed in this thesis. Modeling was done according to the longitudinal dynamics of the linear and non-linear vehicle and the adaptive cruise system was modeled. The vehicle model created was taken as an example of the automatic transmission vehicle model published in matworks. The gas-brake system is designed according to the driver's character. The vehicle was modeled on MATLAB/Simulink and then the controller was designed with the Adaptive Cruise System ACC model. To obtain the transfer function of the system, the transfer function was obtained by the System Identification method with MATLAB/Simulink Tool. The working principle of the genetic algorithm is explained and then applied. While designing the controller of the system, different sources were examined, and the PD controller design was made. Apart from the root locus, which is a manually calculated method, PID tune was made with Genetic Algorithm optimization, which is a machine learning method, for the system to work with a different optimal controller. Finally, the comparison of the controllers was made, and the project was terminated.

Keywords: Automatic Transmission Vehicle Modeling, Longitudinal Vehicle Model, Cruise Systems, Adaptive Cruise Systems, Adaptive Cruise Control, System Identification, Genetic Algorithm

DESIGN, SIMULATION AND EVALUATION OF ADAPTIVE CRUISE CONTROL FOR A VEHICLES

Mustafa TURSUN ve Anıl YILMAZŞAMLI

Kontrol ve Otomasyon Mühendisliği Bölümü

Bitirme Çalışması

Danışman: Dr.Öğr. Üyesi Mumin Tolga EMİRLER

Bu bitirme çalışmasında, seyir sistemleri teknolojilerinden bahsedilmiştir. Seyir sistemlerinin günümüzdeki uygulaması anlatılmıştır. Farklı haberleşme yöntemleriyle sistemin daha geliştirilmesi mümkündür ama bu tezde geleneksel sensörler ele alınmıştır. Lineer ve lineer olmayan aracın boylamsal dinamiklerine göre modellemesi yapıp, adaptif seyir sistemi modellenmiştir. Oluşturulan araç modeli matworks'de yayınlanan otomatik vitesli araç modeli örnek alınmıştır. Gaz-fren sistemi sürücünün karakterine göre tasarlanmıştır. Araç MATLAB/Simulink üzerinde modellenmiş olup daha sonrasında Adaptif Seyir Sistemi ACC modeliyle kontrolcü tasarımı yapılmıştır. Sistemin transfer fonksiyonunun elde edilebilmesi için MATLAB/Simulink Tool'u olan Sistem Tanıma yöntemiyle transfer fonksiyonu elde edilmiştir. Genetik algoritmanın çalışma mantığı anlatılmış olup daha sonra uygulanmıştır. Sistemin kontrolcü tasarımı yapılırken farklı kaynaklar incelenmiş olup PD kontrolcüsü tasarımı yapılmıştır. El ile hesaplanan yöntem olan root locus dışında sistemin farklı bir optimal kontrolcüyle çalışması için makine öğrenmesi yöntemi olan Genetik Algoritma optimizasyonu ile PID tune yapılmıştır. En son kontrolcülerin karşılaştırılması yapıp proje sonlanmıştır.

Anahtar Kelimeler: Otomatik Vitesli Araç Modellenmesi, Boylamsal Araç Modeli, Seyir Sistemleri, Adaptif Seyir Sistemleri, Adaptif Seyir Kontrolü, Sistem Tanıma, Genetik Algoritma

INTRODUCTION

1.1 Literature Survey

While searching the literature, the subject research was carried out in a meticulous order. First of all, it was determined in which field the study would be carried out, and it was decided to conduct research on vehicles. It was decided to develop vehicle software and design a controller. Firstly, a literature research was conducted on vehicle model generation. Research on longitudinal vehicle dynamics was conducted to suit the project. Notation is discussed according to Rajesh Rajamani's Vehicle Dynamics Control book [1], which is the most appropriate source on this subject. Later, research was conducted on cruise systems. Following these researches, research was conducted on cruise control, adaptive systems and autonomous driving technologies used in cruise systems technology. The most suitable design examples for adaptive cruise systems were examined and different controller designs were examined. It has been observed that the most frequently used designs in the literature are PI, PD and PID controllers. PID design is also used in real applications. Methods to obtain optimum coefficients in PID design were examined. A study was conducted on Genetic Algorithm for comparison [2].

1.2 Objective of Study

In recent years, a significant increase in vehicle numbers has been observed along with the rise in the world's population. This surge has propelled vehicle manufacturers into new quests. Nowadays, with the advancement of information and communication technology, innovations in vehicle and driver safety are emerging in the automotive sector. Especially, safety systems in vehicles are among the primary areas of significant investment and attention for manufacturers.

In addition to safety systems, systems focusing more on the comfort of drivers and passengers are also of great importance to manufacturers. Systems that take over the driver's movements during cruise, thereby reducing the driver's physical and mental

fatigue and enabling a healthier response in possible emergencies, are referred to as cruise systems.

A simple example of these systems is the Cruise Control (CC) system. Favored especially for long journeys, this system, once activated by the driver at a desired speed, works to maintain the vehicle's speed at this set value. The system disengages when the gas, brake, or clutch pedals are pressed.

Another cruise system is the Adaptive Cruise Control (ACC) system. These systems, encompassing cruise control, are designed for greater safety. In ACC systems, in addition to the functions of cruise control, the system identifies the vehicle ahead using onboard sensors as the target vehicle and considers its speed as the target speed. Thus, it maintains speed control with the vehicle ahead. ACC systems possess numerous controllers on the engine and brake system, allowing quick response to the acceleration or deceleration of the lead vehicle, automatically adjusting the speed and maintaining a safe distance. If the followed vehicle changes lanes or exits the road, the system reverts to a standard cruise control, maintaining the speed set by the driver.

Smart speed control systems facilitate the task of long-distance drivers and reduce fatigue. Figure 1.1 demonstrates a fatigue-risk graph for long-haul drivers, tested both in a laboratory and on a highway. As the driver's fatigue increases and attention diminishes over time, the risk of accidents also grows. In situations where sudden reaction is needed, such as when an object unexpectedly appears in front of the vehicle or in unclear visibility conditions, these systems are seen as an enhancement to active safety. While in motion, the vehicle travels at the set maximum speed as long as the lane is clear, and maintains a safe distance at the same speed as the vehicle ahead when one is present. If the lane is changed to overtake the vehicle ahead, it automatically accelerates [3].

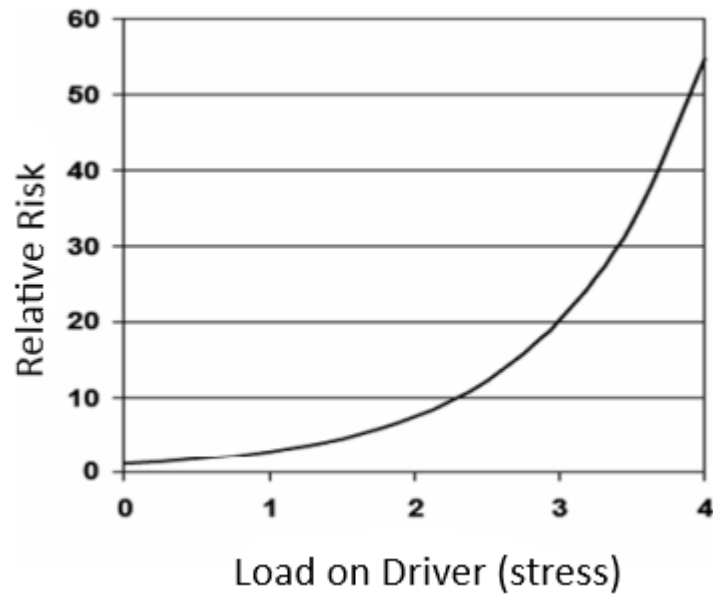


Figure 1.1: A fatigue-risk graph for long tour drivers [4]

In all road and speed scenarios designed to simulate real traffic conditions, it has been observed that the Adaptive Cruise Control (ACC) significantly reduces fuel consumption. The positive impact of ACC, designed for comfort and safety, on fuel consumption is attributed to its ability to control the longitudinal movement of the vehicle at optimal values, independent of various driving characteristics. Compared to vehicles without ACC, the maximum fuel savings were achieved in simulations of speed profiles suitable for slopes as a group. Specifically, on a sloped highway, a variable average speed profile appropriate for the slope resulted in a 16.16% fuel saving in simulations. The lowest savings were typically observed in situations where the vehicle was driven at high speeds with frequent braking. In conclusion, the simulations have been quite successful in representing the real system [5].

Table 1.1: Simulation results summary table: indicates the fuel economy benefits of vehicles with ACC compared to the driver [5]

Simülasyon No	Simülasyon Koşulları			Yakıt Tüketimi Değerleri (gr)			Karşılaştırma (%)
	Yol Eğimi (%)	Ön-Arka Araç Hızı (m/s)	Araçlar Arası İlk Mesafe (m)	Sürücülü Arka Araç	ASS'li Arka Araç	Ön Araç	ASS'nin Sürücüye Göre Avantajı
1	0	6-8 (Sabit)	1000	1098,2	1004,9	900,02	8,50
2	0	10-15 (Sabit)	1000	2860,9	2682,2	1684,7	6,25
3	0	21-23 (Sabit)	600	3853,5	3700,2	3770,6	3,98
4	<8	6-8 (Sabit)	200	3598	3031	2933,4	15,76
5	<6	10-15 (Sabit)	200	3784,4	3448,4	3286,9	8,88
6	<4	21-23 (Sabit)	200	3971,5	3671,2	3695,2	7,56
7	<4	10-15 (Sabit)	200	3421,6	3103	2683,1	9,31
8	0	6-8 (Değişken)	400	1191,1	1131	1106,1	5,05
9	0	10-15 (Değişken)	300	2413,7	2352,2	2532,9	2,55
10	0	21-23 (Değişken)	300	3567,7	3420,7	3581,9	4,12
11	<8	6-8 (Değişken)	200	3399,6	2908,7	2804,3	14,44
12	<6	10-15 (Değişken)	200	4011,6	3564,8	3181,9	11,14
13	<4	21-23 (Değişken)	200	3979,8	3413,5	3579	14,23
14	<4	10-15 (Değişken)	200	3057,6	2563,5	2557,5	16,16

The increase in the number of vehicles registered for traffic, along with factors such as population growth and people's shift towards a more mobile lifestyle compared to previous years, is leading to increased traffic congestion. This situation is directly proportional to the rise in traffic accidents. This increase compels vehicle manufacturers in the automotive sector to invest in safety. As a result of these investments, despite the increase in the number of accidents, a decrease in mortality rates is observed, as shown in Table 1.2 [6].

Table 1.2: The table showing the number of fatal and injury accidents by years [6]

Yıl	Toplam	Ölümlü	Maddi	Ölü sayısı			
	kaza sayısı	yaralanmalı kaza sayısı	hasarlı kaza sayısı	Toplam	Kaza yerinde	Kaza sonrası ⁽¹⁾	Yaralı sayısı
2011	1 228 928	131 845	1 097 083	3 835	3 835	-	238 074
2012	1 296 634	153 552	1 143 082	3 750	3 750	-	268 079
2013	1 207 354	161 306	1 046 048	3 685	3 685	-	274 829
2014	1 199 010	168 512	1 030 498	3 524	3 524	-	285 059
2015	1 313 359	183 011	1 130 348	7 530	3 831	3 699	304 421
2016	1 182 491	185 128	997 363	7 300	3 493	3 807	303 812
2017	1 202 716	182 669	1 020 047	7 427	3 534	3 893	300 383
2018	1 229 364	186 532	1 042 832	6 675	3 368	3 307	307 071
2019	1 168 144	174 896	993 248	5 473	2 524	2 949	283 234
2020	983 808	150 275	833 533	4 866	2 197	2 669	226 266
2021	1 186 353	187 963	998 390	5 362	2 421	2 941	274 615
2022	1 232 957	197 261	1 035 696	5 229	2 282	2 947	288 696

(1) Trafik kazasında yaralanıp sağlık kuruluşuna sevk edilenlerden kazanın sebep ve tesiriyle 30 gün içinde ölenleri kapsamaktadır.

If the benefits of Adaptive Cruise Systems are listed:

Safety Enhancement: Adaptive Cruise Control (ACC) continuously monitors and adjusts the distance and speed between vehicles. This allows vehicles to travel closely yet maintains a safe following distance. If the vehicle in front brakes suddenly, ACC automatically reduces the speed of the following vehicle, thereby reducing the risk of collision. Hence, this system aims to minimize the risk of collisions between vehicles.

Improving Traffic Flow: ACC helps vehicles become more in sync with traffic flow. In heavy traffic, the system automatically adjusts vehicle speeds, reducing congestion. This results in smoother traffic and decreased traffic jams.

Fuel Efficiency: The continuous adjustment of speed and distance between vehicles enhances fuel efficiency. While sudden accelerations and braking can increase fuel consumption, ACC minimizes such maneuvers, leading to fuel savings.

Enhancing Driver Comfort: ACC offers a more comfortable driving experience during long journeys and in traffic. By reducing the need for constant speed and distance adjustments, drivers feel less fatigued, enhancing driving comfort.

Reducing Traffic Accidents: This system aims to reduce traffic accidents caused by driver errors. It continually adjusts the distance between vehicles, especially to prevent rear-end collisions. The system can also compensate for driver inattention or delayed reaction time.

Contributing to Automation and Future Transportation: ACC lays the groundwork for autonomous driving technologies. These systems could enable fully autonomous vehicles in the future, potentially increasing traffic efficiency, preventing accidents, and providing drivers with more comfort and safety.

In conclusion, the adaptive cruise control system aims to achieve significant objectives and goals such as enhancing traffic safety, regulating traffic flow, saving fuel, increasing driver comfort, reducing traffic accidents, and supporting autonomous driving. This system can provide significant contributions to the automotive sector in terms of safety, efficiency, and comfort.

PRELIMINARIES

2.1 Cruise Systems for Vehicles

Systems that take over the driver's movements while driving, reduce the driver's physical and mental fatigue, and thus enable the driver to react more healthily in possible emergency situations while driving, are called cruise systems. These systems are designed to increase both the comfort and safety of the driver while driving. Due to the subject of the thesis, this thesis describes the adaptive cruise system and the controller design for the cruise system.

2.1.1 Cruise Control System

The task of the cruise control system, which means cruise control, is to maintain the set constant speed and reduce pressure of the throttle pedal from the driver. For example, drivers who constantly go on long tours may encounter some physical problems when using the throttle pedal. In this case, the cruise control system provides comfort to the driver. While the vehicle is driving, the driver can continue at a constant speed without pressing the gas. Under normal circumstances, a vehicle; It can adjust the engine speed, wheel rotation speed and how many kilometers per hour it will travel. However, since the cruise control system has the effect to control the throttle, it can control the speed by opening and closing the throttle. For example, if the system is going to travel at a constant speed of 60 kmph, it automatically opens the throttle when it drops below 60 kmph. Then the speed of the vehicle continues to increase until it reaches 60 kmph. However, when the opposite occurs, the throttle is closed and the speed is reduced.

2.1.2 Adaptive Cruise Control for Vehicles

Nowadays, with the developments in automotive technologies, safer, more comfortable and more efficient vehicles are produced. Thanks to these developments, the mechanical systems used in vehicles have been replaced by systems that collect information about the environment and other vehicles with sensors and implement the

outputs of the control system with actuators. With the common use of sensors and actuators in vehicles, driver assistance systems take their place in vehicles. Among the general purposes of these systems; It aims to reduce traffic accidents, improve driving safety, increase transportation efficiency and provide a more comfortable ride by reducing the driving load on the driver. Adaptive cruise systems can be given as an example of these systems. Adaptive cruise systems can be expressed as the first step of autonomous vehicle and smart highway projects. In this system, the vehicle, whose dynamics are handled longitudinally, provides gas, brake and gear control by taking into account the speed limit set by the driver or the speed limit of the road it is on. The system constantly checks the information obtained by the sensors to maintain the speed determined by the driver. In addition, the system allows the vehicle to move automatically by leaving a safe following distance from the vehicle being followed while driving. Since this system does not allowed to control the steering, steering control is performed by the driver during movement. In long-distance driving situations, the driver constantly tries to go at a speed close to the speed limit or the speed driver has determined, and therefore the need to constantly use the gas, brake pedal and gear creates physical fatigue on the driver. This is the reason of this system is especially preferred by long-distance drivers. In the Adaptive Cruise system, while trying to keep the speed constant, the system is disabled when the driver uses with the gas or brake pedal.



Figure 2.1: Waymo full-autonomous taxi [20]

2.1.3 Driving Enhancement

With the developing technology and included it into our lives, it has had many effects that make life easier. This effect is also reflected in vehicles these days. New concepts such as adaptive cruise systems, semi-autonomous driving and fully autonomous driving have been included in daily life. The origin of these technologies began with the invention of the cruise control system. American inventor Ralph Teetor invented a cruise system that allows vehicles to move at a constant speed in 1948. This system was first used in Chrysler brand vehicles in 1958. In the 1980s, Toyota developed laser-based adaptive cruise control. Adaptive Cruise Control (ACC) has become standard for many new vehicles today.

Autonomous driving technology arise in the 2000s and gained great popularity after the 2010s. In 2016, an indie company under the name Waymo implemented the development of autonomous vehicles. In the following years, big brands, especially Tesla, focused on these developments. Developments on automatic parking, smart traffic, cruise systems with cameras, lane tracking, collision avoidance and driverless autonomous vehicles (Autopilot System) are still continuing today.

Thanks to these technologies being developed, it facilitates issues such as reducing possible accidents and ensuring traffic order. Thanks to current issues such as traffic systems working together with autonomous vehicles, traffic explosion can be prevented. It is also of great importance that traffic flow is fast, easy and safe in new urbanization projects. It will be possible to reduce human errors and facilitate transportation thanks to autonomous driving.

2.1.4 General Informations of Cruise Control Systems

Due to the subject of the thesis, cruise and adaptive cruise systems are focused on. The purpose of both systems are provide speed control with gas brake control while driving. However, there are differences between them. The cruise system, unlike the adaptive cruise system, is a system based only on cruise control. It is only adjust the speed of vehicle. The adaptive cruise system is more complex, also provides distance control to the vehicle in front.

2.1.4.1 Basic Principle of Cruise Control

Cruise control is a system that allows vehicles to automatically cruise at a certain speed. Once the driver sets the desired speed, the system automatically controls the accelerator pedal to maintain that speed. When the cruise control system is operating, the amount of gas required to increase or decrease the speed of the vehicle is adjusted electronically with the buttons. In road conditions such as uphill or downhill, the cruise control system increases or decreases engine power to keep the speed constant. The system works through components such as the engine control unit, speed sensors and throttle pedal position sensors. In this way, the driver conformed on long journeys and fuel consumption is optimized. To activate cruise control, it is sufficient to press the button marked in Figure 2.2. Additionally, the fixed speed can be increased or decreased on the right side or deactivated with the "cancel" button at the bottom. In most vehicles, the display is like in Figure 2.2 or very similar.



Figure 2.2: Representation of cruise control button.

2.1.4.2 Basic Principle of Adaptive Cruise Control

The working principle of the Adaptive Cruise System is different from the cruise system, it has a distance and time control. Likewise, this system takes the load off the driver and provides comfort, but does not avoid an accident in an emergency. Therefore, the

Adaptive Cruise System is a driving comfort system. In an emergency situation, when the vehicle suddenly encounters an obstacle, automatic sudden full-braking is another issue. The aim here is to maintain a safe following distance. In daily life, when standards are examined for this, the driver must leave a distance of 2 seconds between the vehicle in front. On grand tours, it may not be possible for the driver to achieve this with full focus and distraction may lead to dangerous situations. For such situations, the adaptive cruise system automatically calculates the safe following time thanks to its distance meter sensor and speed sensor and takes burden away from the driver.

When Adaptive Cruise Systems are examined, it is seen that the parameters that need to be controlled are position and speed. In this system, unless there is a vehicle following in front of the vehicle, the system works like a normal speed controller and ensures that the vehicle continues to move at a constant speed determined by the driver. If a vehicle is in front of the vehicle while driving, the vehicle increases its speed with a certain acceleration if the speed of the vehicle in front is higher than its own speed, according to the speed and position information of the vehicle in front, obtained through sensors, and with a certain acceleration if the speed of the vehicle in front is less than its own speed. It follows the vehicle in front at a safe distance (see Figure 2.3). In cases where the followed vehicle leaves the road or changes lanes, the system automatically works like a classic speed controller and increases the speed of the vehicle with a certain acceleration up to the speed determined by the driver at the beginning, allowing the driver to continue on his way safely. Figure 2.3 shows the operation of the adaptive cruise system.

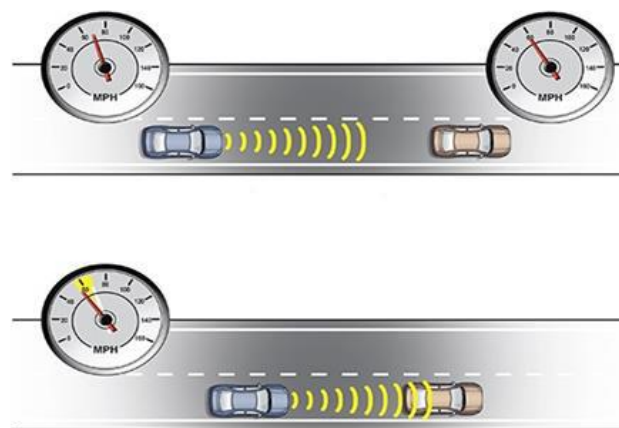


Figure 2.3: Working principle of the ACC [7]

2.2 Control Problem of the ACC for Vehicles

For the requirement of an Adaptive Cruise Control system, the vehicle who following the vehicle in front (Ego) receives speed and location information through sensors. This process aims to prevent violation of the safe distance between vehicles. The controller must fulfill its function as quickly as possible. The safe following methods between vehicles should be no more than 2 seconds. Methods for calculating the distance between two vehicles are explained in the next subsections.

2.2.1 Distance Control of Two Vehicles

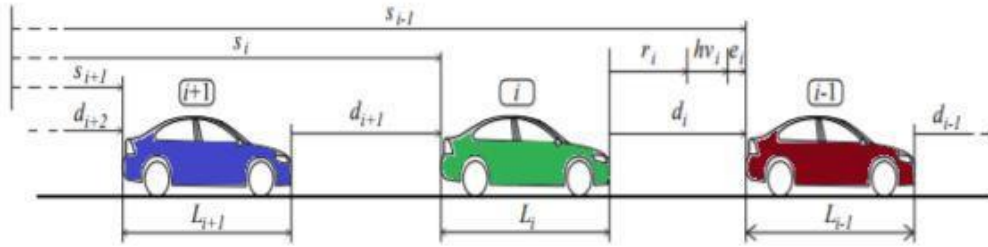


Figure 2.4: Distance representation between the vehicles [19]

For the methods of the distance control, different methods are used to adjust the safe distance between two vehicles. These methods operate according to a constant time and constant distance interval. These methods are mentioned in the following subheadings in 2.2.1.1 and 2.2.1.2.

2.2.1.1 Constant Distance Method

The constant following headway method is actually a subset of the constant following time method, which is considered as $t_{ts,i} = 0$ seconds. Mathematical representation expressed as

$$d_{r,i}(t) = s_i \quad (2.1)$$

The constant following headway method can not be used in real applications because the range needs to be changed according to vehicle speed.

2.2.1.2 Constant Time Headway Method

In the Constant Time Headway method, the safe distance between vehicles varies in direct proportion to the speed of the vehicle in front. As the speed of the vehicle in the lead increases, the safe following distance between them increases. Mathematical representation of the Constant Time Headway,

$$d_{r,i}(t) = s_i + t_{ts,i} \cdot v_i \quad (2.2)$$

Here, s_i is the desired safe position difference when the vehicle is stationary, v_i i-th shows the speed of the vehicle and $t_{ts,i}$ shows the tracking time. Tracking time is defined as the time required for vehicle number i to reach the location of vehicle number i-1 while traveling at constant speed.

In adaptive cruise systems, a control signal is sent based on the information from the sensors for distance and speed control. Thanks to the ACC system, the vehicle behind (Ego) leaves a safety distance equal to the minimum time limit. About the simple calculation of this distance, if two vehicles are traveling at a constant speed of 100 kmph, the distance between the two vehicles should be minimum 100 kmph x 2 seconds, that is equal to 200 meters.

2.3 Genetic Algorithm

Evolutional algorithm is a machine learning method that mimics the process of natural selection and provides optimization for systems. A population of individuals, called a generation, compete at a given task with a well-defined cost function, and there are rules to propagate successful strategies to the next generation. Because the information processed in many processes is so large, there may be more than one output. Therefore gradient search algorithms may yield sub-optimal results. Evolutionary algorithms provide an effective alternative search strategy for finding near-optimal solutions in a high-dimensional search space.

Random values or predetermined data sets can be used as initial generation. Initially, the first generation is created in random order and their performance is evaluated according to a cost function. An individual in a genetic algorithm corresponds to a set of parameter values in a model with parameters to be optimized; this parameterization is

shown in Figure 2.5. In genetic programming the individual corresponds to the structure of the control law and certain parameters

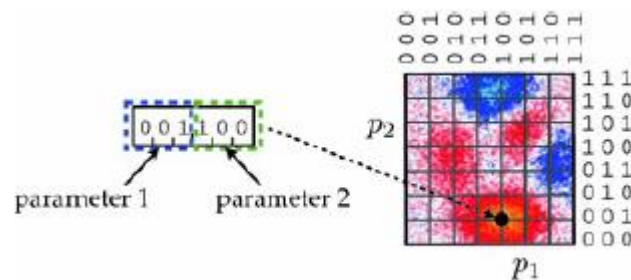


Figure 2.5: Representation of an individual (parameter) in genetic algorithms. This binary representation encodes two parameters that are each represented with a 3-bit binary expression. Each parameter value has an associated cost (right), with red indicating the lowest cost solution [2]

Once the first generation is populated with individuals, each is evaluated and assigned a fitness based on their performance on the cost function metric. Individuals with a lower-cost solution have higher fitness and are more likely to pass on to the next generation. There are a set of rules, or genetic operations, that determine how successful individuals progress to the next generation:

Elitism: a few of the fittest individuals pass directly to the next generation. Elitism ensures that the top individuals of each generation remain intact without noise.

Replication: Individuals pass directly to the next generation based on their fitness; It is also called asexual reproduction in genetic programming.

Crossover: Two individuals are selected based on their fitness and random portions of their parameters are exchanged. These two individuals move forward with the exchanged information.

Mutation: Individuals proceed with random parts of the parameter representation replaced by new random values.

Population: In a genetic algorithm, a population consists of a set of individuals, each representing a possible solution to a problem. These individuals are typically encoded as strings of genes, which collectively form what is called a chromosome. The population size, which can vary depending on the specific requirements of the algorithm or problem, directly influences the genetic diversity available for developing robust

solutions. The algorithm iteratively modifies the population through processes modeled on natural evolution, such as selection, crossover, and mutation.

Generation: A generation in a genetic algorithm refers to one complete cycle of processes that create a new set of individuals (a new population) from the current set. Each generation involves selecting the fittest individuals from the current population, applying genetic operators like crossover and mutation to generate new offspring, and then replacing the older population with this new one. The concept of generations is fundamental in genetic algorithms as it tracks the progression of evolving solutions. The number of generations is a key parameter that determines how long the algorithm runs and significantly affects the quality of the solution, with more generations typically allowing for a more thoroughly explored solution space.

Mutation serves to explore the search space and provides access to global minima, while crossover optimizes locally using successful structures. Successful individuals from each generation are passed on to the next generation through these four genetic operations. New individuals can be added to each generation to add diversity. This is shown schematically in Figure 2.6 for the genetic algorithm. Generations evolve until performance reaches the desired stopping criterion.

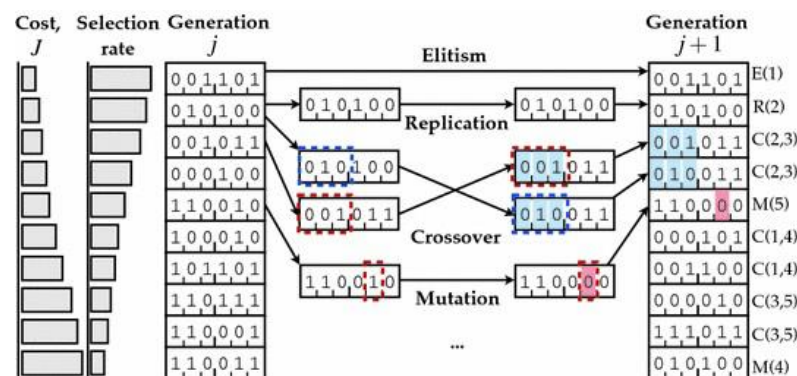


Figure 2.6: Genetic operations to advance one generation of parameters to the next in a genetic algorithm [2]

About Figure 2.6 The probability of an individual from generation j being selected for generation is related inversely to the cost function associated with that individual. The genetic operations are elitism, replication, crossover, and mutation.

It is possible to increase the number of generations and the population to improve the performance of evolutionary algorithms. It can be used to set parameters in control applications. PID applications can be an example of this.

2.4 Hardwares for ACC

In order for cooperative adaptive and adaptive cruise systems to work properly, hardware such as sensors, actuator hardware and in-vehicle controller hardware are needed.

Longitudinal sensors such as RADAR (Radio Detection and Ranging) and LIDAR (Light Detection and Ranging) are used in vehicles to ensure a safe distance and smooth driving. In addition to these sensors, camera systems are also used in vehicles with the development of image processing technology. Their advantages and disadvantages compared to each other can be mentioned. The lens of the lidar sensor sends and collects optically adjacent laser beams. The most important advantage of this sensor compared to others is its low price and easy placement in the vehicle. Another advantage of lidars is that they have a multi-scanning function [8]. In this way, they can distinguish more than one object at the same time. However, the laser beams sent and received by the sensor are very sensitive to environmental conditions. For this reason, measurements of this sensor are not reliable in cases such as bad weather conditions or fog. That's why manufacturers in the automotive industry use radar sensors as well as lidar sensors in vehicles.

In adaptive cruise systems, the interaction of the vehicle with the environment is provided by the radar, which is the main component of the system. Radar is used to detect the distance and relative speed of the vehicle to the vehicles in front of it while driving. Although there are a wide variety of radars used in cruise systems and based on different physical principles, two types of radars generally stand out. The first of these is the long-range millimeter wave radar. This type of radar detects objects within its range using the Doppler effect. The system sends the sine signal at a certain frequency within the millimeter wave range with a signal source and receives it back with the help of a signal receiving antenna. Meanwhile, the time between the signal hitting the object

it encounters within the range, being reflected back from there, and reaching the radar again is defined as flight time.

This period is found by,

$$t_{flight} = \frac{2d}{c} \quad (2.3)$$

Here, d represents the distance to be measured and c represents the speed of light. This flight time obtained gives the distance after taking into account the speed of the vehicle. The Doppler effect obtains the relative speed of the object in front of the vehicle by using the wavelength difference between the outgoing and incoming signals. As can be seen in Figure 2.7, if the vehicle sending the radar signal approaches or moves away from the target, a change in the frequency value of the sent radar signal is observed. For example, if the speed of the vehicle being followed is lower than the speed of the system, there will be a frequency difference in the signal sent by the radar.

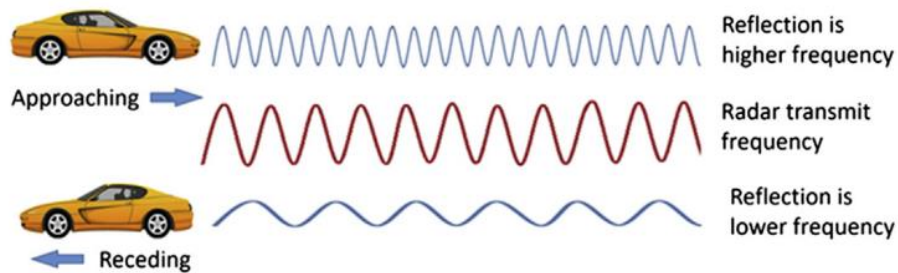


Figure 2.7: Doppler effect [9].

By measuring this difference value, the speed difference between the vehicles is obtained. This calculated speed difference value is transmitted to the system and the speed of the vehicle is slowed down with a certain acceleration and the safe distance is controlled.

MATHEMATICAL MODELING OF THE VEHICLE

In this part of the thesis, linear and non-linear vehicle modeling is mentioned. The methods used in modelling are explained under separate heading.

3.1 Linear Modeling for Longitudinal Dynamics

First of all, the vehicle dynamics should be examined longitudinally to create a realistic physical model. With the mathematical model of the vehicle obtained with these dynamics, we can easily create the system and design the controller of this system. Obtaining a physical model is important in determining the method to be used.

When looking at the longitudinal dynamics of the vehicle, the resulting equations and parameters are shown as follows in Figure 3.1.

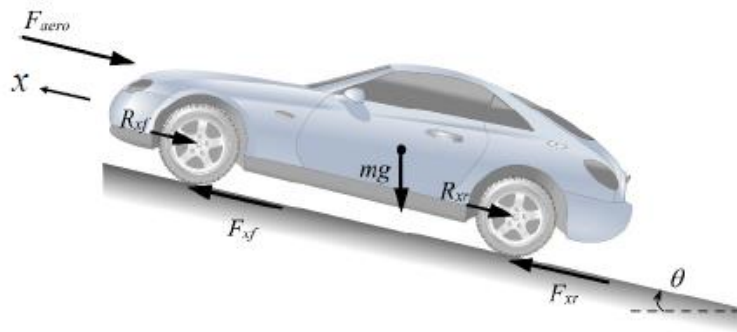


Figure 3.1: Longitudinal forces applied moving car on a inclined road [1].

A force balance along the vehicle longitudinal axis yields [1]

$$m\ddot{x} = F_{xf} + F_{xr} - F_{aero} - R_{xf} - R_{xr} - mg \sin \theta \quad (3.1)$$

3.1.1 Aerodynamic Drag Force

Aerodynamic drag force, also known simply as drag, is a resistance force that acts opposite to the direction of motion of a vehicle as it moves through the air. This force is a crucial factor in the study of vehicle dynamics and plays a significant role in determining the efficiency and performance of a vehicle. Aerodynamic Drag Force equation can be written as [1],

$$F_{aero} = \frac{1}{2} \rho C_d A_F (V_x + V_{wind})^2 \quad (3.2)$$

3.1.2 Longitudinal Tire Force

The frictional forces F_{xf} and F_{xr} , acting on the front and rear tires respectively, are generated by the interaction with the ground, constituting the longitudinal tire forces as seen in Figure 3.1.

Experimental findings have confirmed that the amount of longitudinal force each tire produces is influenced by the slip ratio, the vertical load on the tire, and the friction coefficient at the tire-road surface. The vertical force exerted on a tire is known as the tire's normal load. This load originates from a portion of the vehicle's weight and is affected by the vehicle's center of gravity location, longitudinal acceleration, aerodynamic drag, and the incline of the road.

Slip Ratio: Longitudinal slip refers to the discrepancy between the wheel axle's actual longitudinal velocity V_x and the tire's effective rotational velocity, which is r_{eff} multiplied by ω_w . Essentially, longitudinal slip is the difference between $r_{eff}\omega_w$ and V_x . Longitudinal slip ratio is defined as

$$\sigma_x = \frac{r_{eff}\omega_w - V_x}{V_x} \quad (\text{during braking}) \quad (3.3)$$

$$\sigma_x = \frac{r_{eff}\omega_w - V_x}{r_{eff}\omega_w} \quad (\text{during acceleration}) \quad (3.4)$$

3.1.3 Rolling Resistance

Generally, the rolling resistance is conceptualized as being approximately proportional to the normal force acting on each set of tires, that is to say [1].

$$R_{xf} + R_{xr} = f(F_{zf} + F_{zr}) \quad (3.5)$$

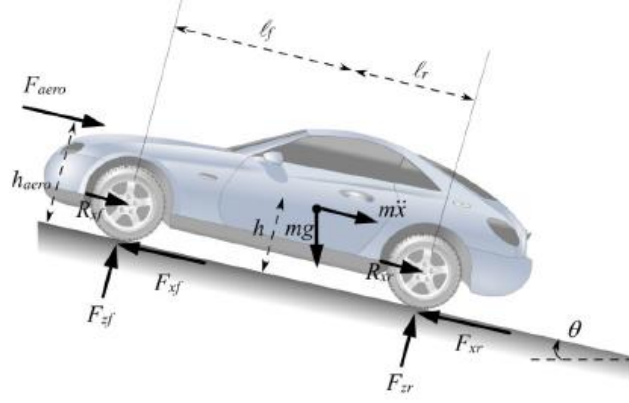


Figure 3.2: Dynamic representation of the vehicle in inclined road [1]

For Figure 3.2, It represents the dynamic representation of the vehicle when it moves on a two-dimensional, inclined road and the distances between the tires are added [1].

$$F_{zf} = \frac{-F_{aero}h_{aero} - m\ddot{x}h - mgh \sin \theta + mg\ell_r \cos \theta}{\ell_f + \ell_r} \quad (3.6)$$

$$F_{zr} = \frac{F_{aero}h_{aero} + m\ddot{x}h + mgh \sin \theta + mg\ell_f \cos \theta}{\ell_f + \ell_r} \quad (3.7)$$

The distribution of the normal force on the tires can be calculated by presuming that the vehicle's overall pitch torque is neutral. This implies that the vehicle's pitch angle is considered to have stabilized at a constant value.

3.1.4 Upper Level Controller

According to the Upper Level Controller Scheme shown in Figure 3.3, the upper-level controller detects the relative distance of the vehicle. It uses information from sensors to calculate this velocity.

Let v_l and v_f are respectively the velocity of leader vehicle and ego vehicle with the desired is to make the speed $v_f \triangleq v_l$. As such v_l is the desired velocity trajectory is to be tracked by the follower vehicle [10]

$$\delta_f = \Delta v = v_l - v_f \quad (3.8)$$

The desired inter-vehicle distance between the leader to ego vehicle is not constant but varies linearly with velocity and it is defined as [10]

$$d_{ref} = r_0 + h \cdot v_f \quad (3.9)$$

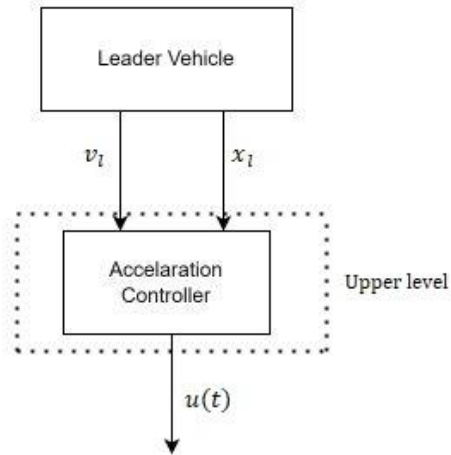


Figure 3.3: The Upper Level Controller Scheme

3.2 Nonlinear Modeling for Longitudinal Dynamics

In the nonlinear model, the vehicle dynamics equations are the same as the linear vehicle model for the upper level. Therefore, the previously written should be looked at in Section 3.1 equation (3.1).

In this section, unlike the linear vehicle, the vehicle's powertrain, engine, wheels and braking system will be covered. As shown in Figure 3.4, the entire block model of the vehicle can be seen and the block diagram seen in Figure 3.5 explains the power-load exchange between the engine, torque converter drivetrain and wheels.

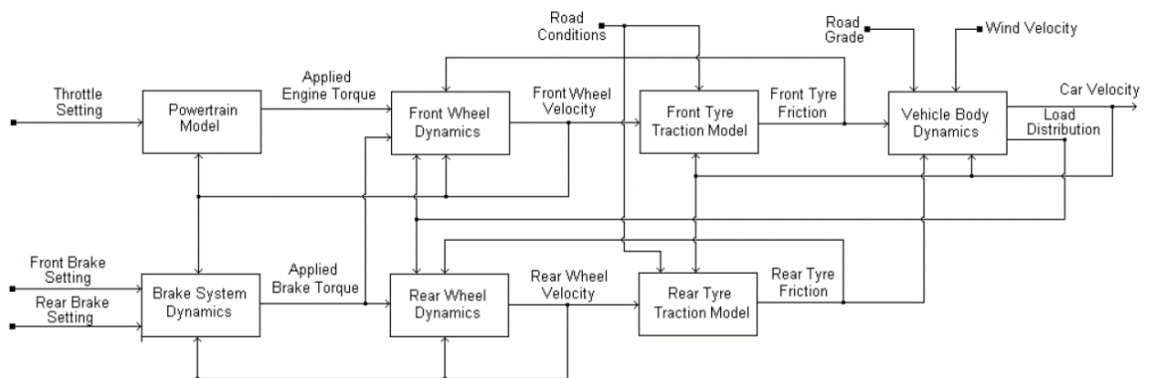


Figure 3.4: Vehicle System Block Structure [11]

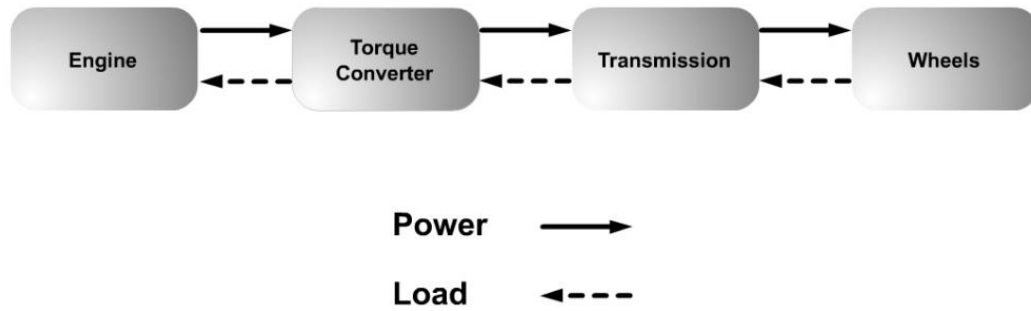


Figure 3.5: Power flow and loads in vehicle drivetrain [1]

3.2.1 Lower Level Controller

In this section, the lower dynamics of the vehicle will be discussed. In the subsections, the vehicle's engine, tire dynamics, torque converter and transmission dynamics will be discussed. Unlike the linear vehicle, the controller will now be designed for the non-linear vehicle, so the equations here are given briefly. Since determining the parameters in these equations enters into the design of a vehicle which it is another topic for the mechanical engineering, the parameters are quoted from a different source [12].

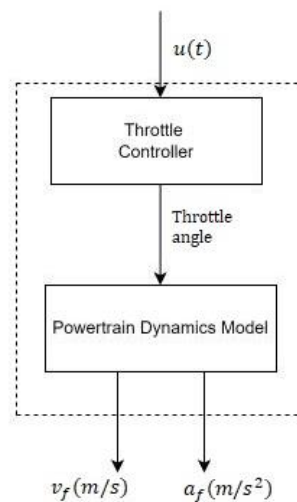


Figure 3.6: This block model shows the outputs from the powertrain and engine according to the throttle pedal angle.

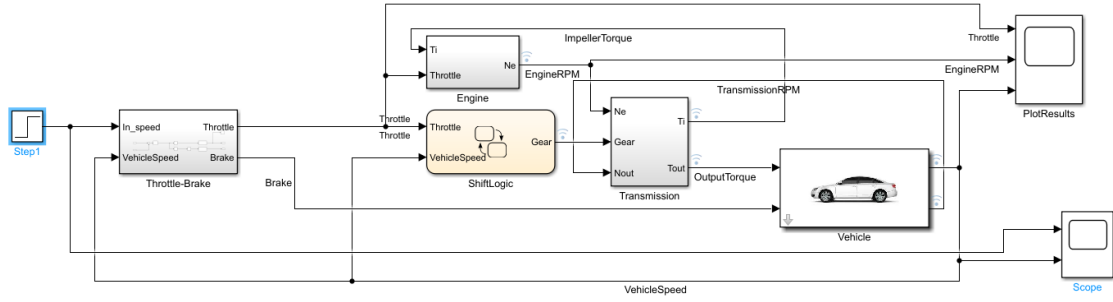


Figure 3.7: Simulink model of the Auto Transmission vehicle and include driver characteristic for control the throttle.

The model created by combining the subsystems included in the vehicle dynamics is shown in Figure 3.7. In order for the model to work, inputs are added to the model as percentage throttle opening and brake torque. A delayed transfer function is used within the system to take into account the delay after applying the brakes. In this way, a more realistic brake model approach was achieved.

3.2.1.1 Engine of the Vehicle

The engine rotational speed dynamics can be described by the equation [1]

$$I_e \dot{\omega} = T_i - T_f - T_a - T_p \quad (3.10)$$

where T_i is the engine combustion torque, T_f are the torque frictional losses, T_a is the accessory torque and T_p is the pump torque and represents the load on the engine from the torque converter.

Using the notation [1]

$$T_e = T_i - T_f - T_a \quad (3.11)$$

to represent the net engine torque after losses, we have [1]

$$I_e \dot{\omega}_e = T_e - T_p \quad (3.12)$$

The net engine torque T_e depends on the dynamics in the intake and exhaust manifold of the engine and on the accelerator input from the driver.

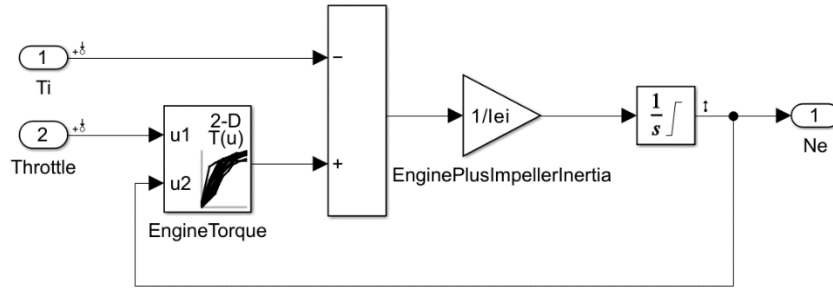


Figure 3.8: Inside of the engine model for vehicle and look-up table for engine torque characteristic map.

This model shows the effect of the torque added by an impeller and the position of the throttle on the speed of the engine. The result is N_e , the rotational speed of the motor at any given time, and with this value the instantaneous power or performance status of the motor can be understood.



Figure 3.9: Block representation of engine inertia model [1]

$$I_{ei}\dot{N}_e = T_e - T_i \quad (3.13)$$

3.2.1.2 Transmission of the Vehicle

Denoting the gear ratio of the transmission as R , it is contingent upon the operational gear and encompasses the ultimate gear reduction within the differential assembly. Typically, R exceeds unity ($R > 1$), with a propensity to augment upon upshifting. T_t represent the input torque to the transmission, and T_{wheels} signify the torque transmitted to the wheels. During sustained operation across various gears of the transmission, the torque conveyed to the wheels can be expressed as:

$$T_{wheels} = \frac{1}{R} T_t \quad (3.14)$$

The relation between the transmission and wheel speeds is

$$\omega_t = \frac{1}{R} \omega_w \quad (3.15)$$



Figure 3.10: Block representation of transmission model [1]

The consistent gear ratio R at a steady state is contingent upon the current operational gear. The selection of this operational gear is dictated by a predetermined gear shift schedule, which is influenced by both the speed of the transmission shaft and the extent of throttle opening.

Replace equations (3.14) and (3.15) by the following 1^{st} order equations during a gear change:

$$\tau \dot{T}_{wheel} + T_{wheel} = \frac{1}{R} T_t \quad (3.16)$$

$$\tau \dot{\omega}_t + \omega_t = \frac{\omega_w}{R} \quad (3.17)$$

Equation (3.16) is initialized with wheel $T_{wheel} = 0$ at the instant that the gear change is initiated. R is the gear ratio at the new gear into which the transmission shifts. ω_t is initialized at $\frac{1}{R_{old}} \omega_w$ where R_{old} is the old gear ratio [1].

The gear change is assumed to be complete when T_{wheel} and ω_t converge to $\frac{1}{R} T_t$ and $\frac{\omega_w}{R}$ within a threshold value. Once the gear change is complete, in (3.14) and (3.15) can be used again to represent the transmission [1].

In modeling the transmission, the transmission ratio and torque converter blocks are used as subsystems in the model. The torque converter model will be explained as a separate heading. In this section, the gear shifting algorithm is also mentioned. This

model is used to obtain how the transmission converts engine torque and speed in different gears and its effect on vehicle motion.

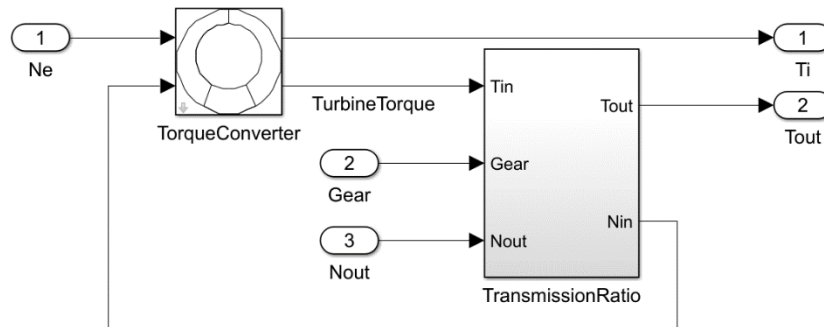


Figure 3.11: Inside of the transmission block for auto transmission vehicle and also include torque converter.

The torque converter model is to show how engine speed and torque are changed through the torque converter and converted into turbine torque. The torque converter allows the engine to deliver maximum torque across a constant speed range, while ensuring the transmission delivers torque effectively at lower speeds. This is especially important when starting off and maneuvering at low speeds.

Engine speed (N_e) enters the torque converter where it is associated with impeller speed (N_{in}). Speed ratio (SpeedRatio) and torque ratio (TorqueRatio) govern the power transfer from the impellers to the turbine. These ratios are based on data obtained from lookup tables (1-D Lookup Tables) that determine the efficiency and output characteristics of the torque converter. The torque converter converts the torque (T_i) produced by the engine into torque (T_t) transferred to the turbine and applies it to the input of the transmission. This process allows the engine torque and speed to be adjusted to suit the transmission requirements, thus using the engine's power in the most efficient way and improving the vehicle's acceleration and starting performance.

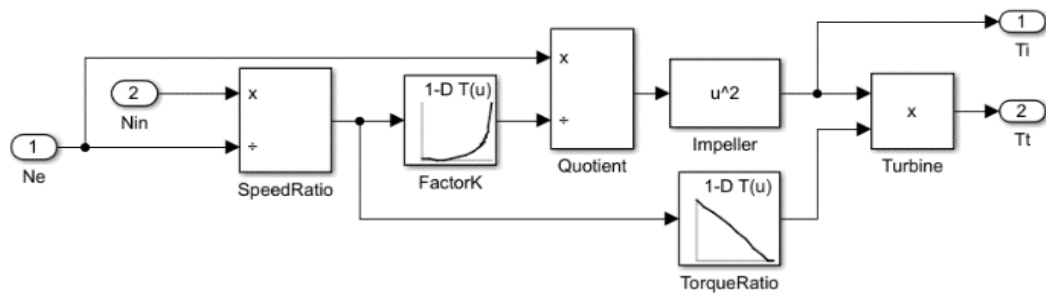


Figure 3.12: Subsystem of the torque converter

The gear ratio model you see in Figure 3.13 shows how the input torque (T_{in}) is processed through the transmission and transformed into the output torque (T_{out}), as well as how the input speed (N_{in}) is converted to the output speed (N_{out}). The "1-D Lookup Table" within the model defines the gear ratio and torque conversion for the selected gear ("Gear"). This table illustrates the impact of each gear ratio on torque. As a result, using these ratios, the engine's torque and speed are transformed into the torque and speed values at the transmission output. This model aids in understanding the vehicle's dynamic behavior and performance, simulating how optimal torque and speed can be maintained during gear shifts.

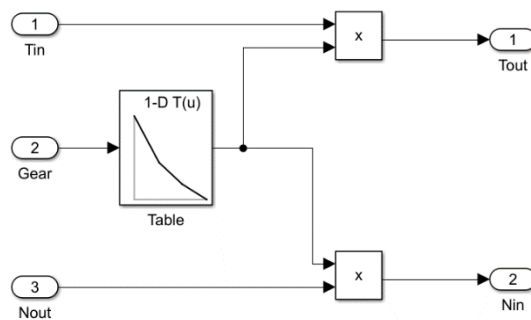


Figure 3.13: Subsystem of the TransmissionRatio block. The look-up table for gears and gear ratio for 4-gear forward vehicle.

Engine torque first enters the torque converter where it is converted into turbine torque in Figure 3.11. This process allows the engine's rotational speed to be adapted to the needs of the transmission. The shift block inside the model represents which gear is active and determines how torque and speed are transmitted to the transmission output in Figure 3.15. The transmission ratio block converts engine speed to transmission output speed in a given gear. As a result, the model calculates the transmission output torque and speed in accordance with the selected gear and transmission ratio, which are output parameters that affect the acceleration and overall performance of the vehicle in Figure 3.16.

Table 3.1: Transmission gear rates.

nth Gear	Gear Ratio (R_{TR})
1	2.393
2	1.450
3	1.000
4	0.677

$$T_i = \frac{N_e^2}{K^2} \quad (3.18)$$

$$K = f_2 \frac{N_m}{N_r} = K - factor(capacity) \quad (3.19)$$

$$R_{TQ} = f_3 \frac{N_m}{N_e} = torque\ ratio \quad (3.20)$$

The transmission model is implemented via static gear ratios, assuming small shift times in (3.21) and (3.22)

$$T_{out} = R_{TR} T_{in} \quad (3.21)$$

$$N_{in} = R_{TR} N_{out} \quad (3.22)$$

The final drive, inertia, and a dynamically varying load constitute the vehicle dynamics in (3.23) and (3.24).

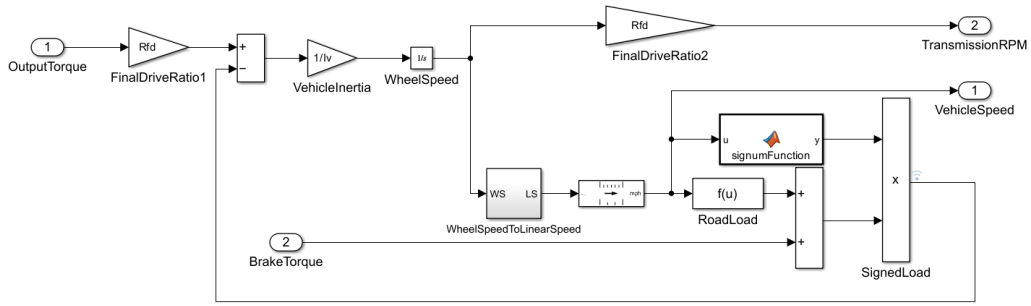


Figure 3.14: Subsystem of the vehicle block.

This vehicle dynamics model in Figure 3.14, simulates the process of converting the output torque produced by the engine and the effects of braking torque into the vehicle's wheel speed and transmission rpm. In the model, the output torque is multiplied by two separate final drive ratios; the first is used to convert torque into wheel speed, and the second is used to convert wheel speed into transmission RPM. Vehicle inertia is also taken into account in this transformation. Additionally, the impact of factors such as road load, wind resistance and slope on the vehicle is adjusted according to the direction of the load using a sign function and included in the vehicle speed, which represents the actual speed of movement of the vehicle. This model enables a detailed analysis of the performance of the vehicle by providing a comprehensive analysis of the internal and external factors affecting the vehicle movement dynamics

$$I_v \dot{N}_w = R_{fd}(T_{out} - T_{load}) \quad (3.23)$$

$$T_{load} = f_5(N_w) = load\ torque \quad (3.24)$$

The load torque includes both the load and brake torque. The road load is the sum of frictional and aerodynamic losses in (3.25)

$$T_{load} = sgn(mph)(R_{load0} + R_{load2}mph^2 + T_{brake}) \quad (3.25)$$

The model programs the shift points for the transmission according to schedule shown in the figure below in Figure 3.15. For a given throttle in a given gear, there is unique

vehicle speed at which an upshift takes place. The simulation operates similarly for a downshift [12].

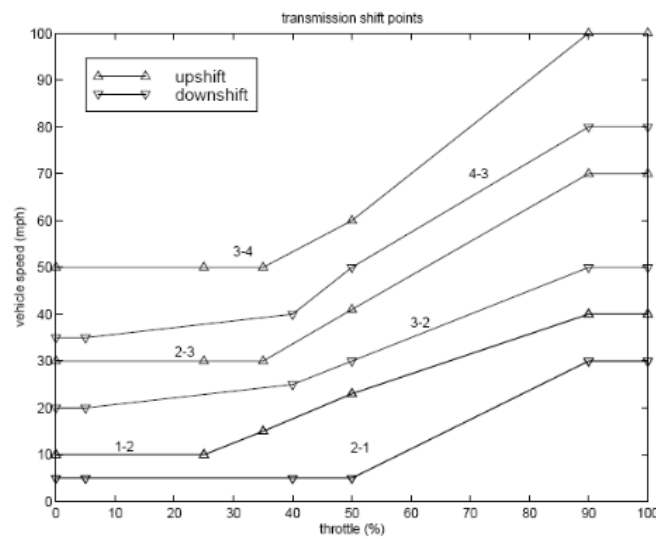


Figure 3.15: Relation between speed-throttle and shifting points [12]

In the model used, the transmission applies the shift points according to the program shown in Figure 3.15. For a specific throttle opening at a given gear, there exists a vehicle speed threshold at which an upshift occurs, initiating the transition to the next gear. Similarly, the simulation operates for downshifting, where a certain lower speed threshold dictates the change to a lower gear.

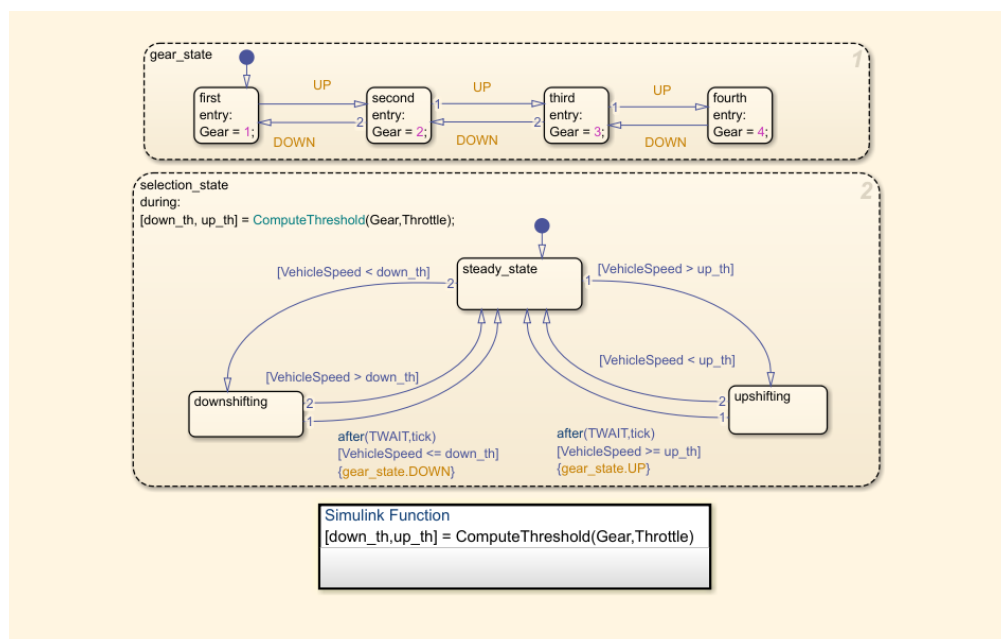


Figure 3.16: 4-gear vehicle shifting algorithm in Simulink

In adaptive cruise systems, vehicles must have automatic transmission. The state flow diagram in Figure 3.16 above governs the gearshift timing of the transmission. It starts with a 'gear_state' which determines the current gear state of the transmission, and then there is a 'selection_state' which calculates certain speed thresholds based on the throttle position and current gear. When the vehicle is in a steady state ('steady_state'), the gear is lowered and increased according to the speed thresholds: if the vehicle's speed is higher than the up threshold, the gear is increased, if it is lower than the lower threshold, the gear is lowered. This mechanism allows the transmission to shift gears smoothly in accordance with the vehicle speed and the driver's throttle input.

3.2.1.3 Wheel Dynamics of the Vehicle

For the driving wheels (for example, the front wheels in a front-wheel driven car), the dynamic equation for the wheel rotational dynamics is [1]

$$I_w \dot{\omega}_{wf} = T_{wheel} - r_{eff} F_{xf} \quad (3.26)$$

where ω_{wf} , T_{wheel} and r_{eff} have been defined earlier and F_{xf} is the longitudinal tire force from the front wheels.

For the non-driven wheels [1]

$$I_w \dot{\omega}_{wr} = -r_{eff} F_{xr} \quad (3.27)$$

where F_{xr} is the longitudinal tire force from the rear wheels



Figure 3.17 Block representation of wheel inertia dynamic

The total longitudinal tire force is given by [1]

$$F_x = F_{xf} + F_{xr} \quad (3.28)$$

Each of the two tire force terms F_{xf} and F_{xr} is a function of the slip ratio at the front and rear wheels respectively. For calculation of the slip ratio at the front wheels, ω_{wf} should be used, while for the calculation of the slip ratio at the rear wheels ω_{wr} should be used.

3.2.1.4 Throttle-Break Characteristic of the Vehicle

A driver behavior module is necessary to enhance the realism of the vehicle, as it is not fully automated. A block has been designed to control the signals sent to the gas and brake pedals. This block moderates any excessive effects of the speed signal received at the input, and works in conjunction with the PI control of the vehicle's exit speed at the output. A PID tuner was used to optimize the response. The inputs to both pedals are transmitted as percentages. To add realism to the gas pedal response, a small delay transfer function has been incorporated.

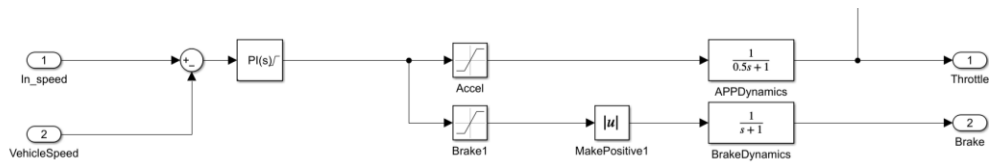


Figure 3.18: Throttle Brake Subsystem

3.3 Safe Distance Control

In this technique, the appropriate distance to maintain between vehicles changes in proportion with the vehicle's speed; Thus, as the vehicle picks up pace, the space to the vehicle ahead increases accordingly. The equation representing the separation between two vehicles in this technique is symbolized by

$$d_{r,i}(t) = r_i + h \cdot v_i(t) \quad (3.29)$$

In the constant following time method, the desired safe distance between vehicles varies in direct proportion to the speed of the vehicle, that is, as the vehicle accelerates, the distance between it and the vehicle in front increases.

In this method, the mathematical representation of the distance between two vehicles is expressed as

$$d_{r,i}(t) = s_i + t_{ts,i} \cdot v_i \quad (3.30)$$

Here, r_i is the desired safe position difference when the vehicle is stationary, v_i is i . indicates the speed of the vehicle and h indicates the time headway. The tracking time is defined as the time required for vehicle number i to reach the location of vehicle number $i-1$ while traveling at constant speed.

The distance d_i between two cars should be expressed as the difference of the absolute positions of the cars. The absolute position s_i of a car is defined as the position of the rear bumper of the car. With these definitions, the distance error $e_i(t)$ can be defined as:

$$e_i(t) = d_i(t) - d_{r,i}(t) \quad (3.31)$$

$$e_i(t) = (s_{i-1}(t) - s_i(t) - L_i) - (r_i + h \cdot v_i(t)) \quad (3.32)$$

Here L_i i -th shows the length of the vehicle. However, in writing this thesis, vehicle dimensions were taken as $L_i = 0$. The vehicle is accelerated or decelerated according to the error signal obtained as a result of the operations in (3.32) [7].

ADAPTIVE CRUISE CONTROL MODELING

4.1 Estimation of Transfer Function

To describe the system, the closest possible transfer function or an exactly obtained transfer function is needed. This system obtained with dynamic parameters or by using the output response of an existing system.

It is easier to make a close estimation for the linear system of the vehicle based on its longitudinal dynamics alone, but it is not possible to estimate the transfer function of the nonlinear system. To estimate the transfer function of a nonlinear system, it can be found using the System Identification Toolbox program in MATLAB. This subject will be discussed in more detail in the next chapter (see Section 4.1.1).

Using only the longitudinal dynamics for the transfer function (represented as $G_i(s)$) of a linear system given a acceleration input, it can be said that the system looks like this

$$G_i(s) = \frac{X_i(s)}{U(s)} = \frac{1}{s} \cdot \frac{1}{s} \cdot \frac{1}{(\tau_i s + 1)} = \frac{1}{s^2(\tau_i s + 1)} \quad (4.1)$$

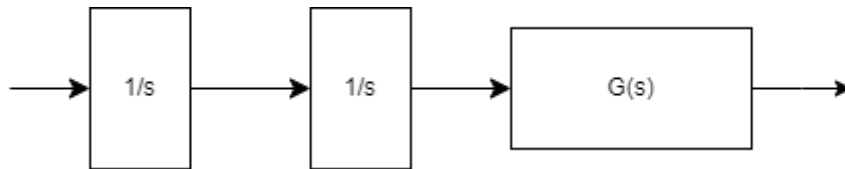


Figure 4.1: Open-Loop system representation with acceleration input.

4.1.1 System Identification Toolbox

System Identification Toolbox™ provides MATLAB® functions, Simulink® blocks, and an application for dynamic system modeling, time series analysis, and forecasting. When using time or frequency domain data, dynamic relationships between measured variables can be found to create transfer functions, process models, and state-space models in continuous or discrete time. AR can predict time series using ARMA and other linear and nonlinear autoregressive modeling techniques.

The toolbox allows to estimate nonlinear system dynamics using Hammerstein-Wiener and Nonlinear ARX models with machine learning techniques such as Gaussian Processes (GP), Support Vector Machines (SVM), and other representations. Alternatively, neural ordinary differential equation (ODE) models can be created using deep learning to capture nonlinear system dynamics. The toolbox enables gray-box system definition to estimate the parameters of a user-defined model. Defined models can be integrated into Simulink for rapid simulations to enable control design, diagnostic and prognostic applications [13].

To use this helper function, which is used to find the transfer function of the vehicle, first of all, by giving the system a constant speed (step signal or constant), the system output data is defined in MATLAB via Simulink. Later, when `systemIdentification` is typed in the "command window" section, an estimated transfer function can be obtained by identifying the outputs of the system in the window that opens. Velocity response in Figure 4.2 of the nonlinear vehicle will be used for estimate the system.

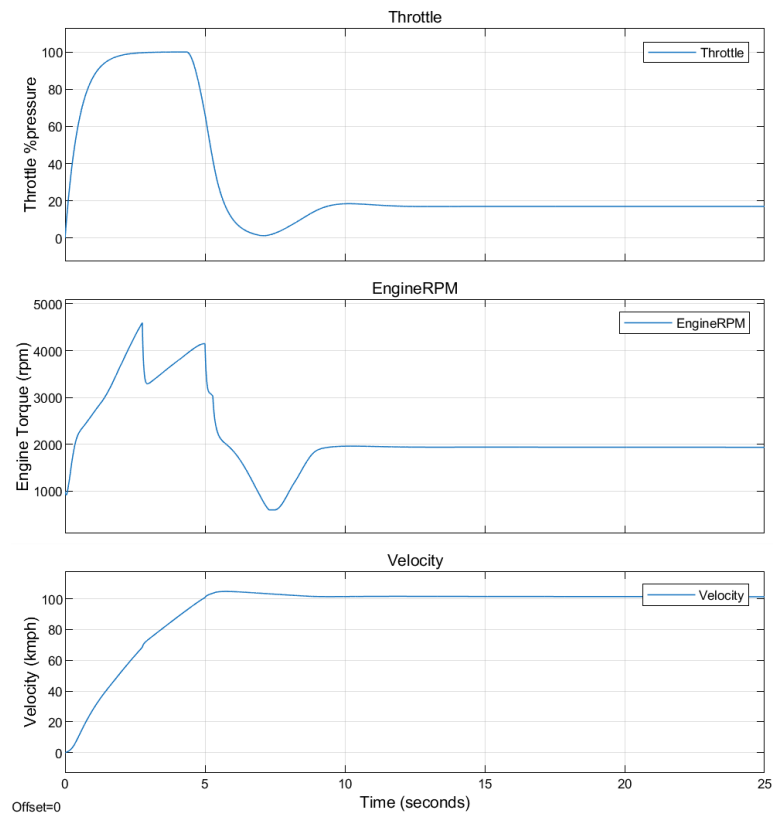


Figure 4.2: Output of the Nonlinear Vehicle in order Throttle Pressure, Engine Torque and Velocity. This response get from constant 100 kmph as input.

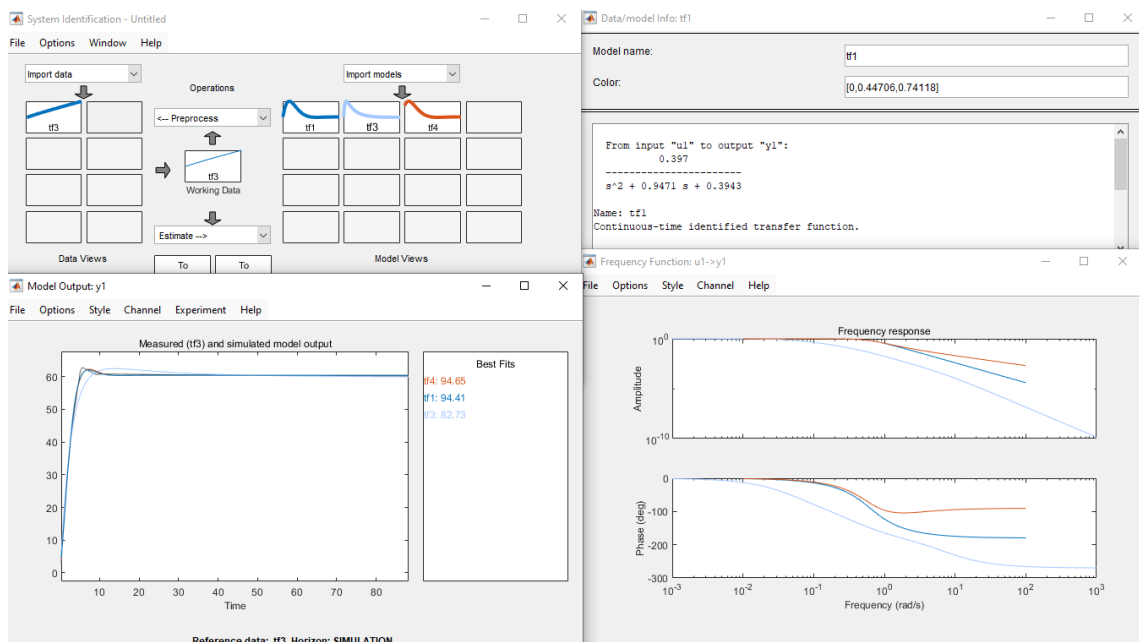


Figure 4.3: System Identification of Nonlinear Vehicle

When defining the system, it is known approximately what the transfer function might be like. When defining the system, first three transfer functions are defined, which are a non-zero one pole (light blue), a non-zero two pole (dark blue) and a one zero two pole (orange) point. By entering this information into the System Identification Tool, asked to make a prediction based on the step answer. As a result, 83%, 94.41% and 94.65% success predictions are obtained, respectively as in Figure 4.4. From these predictions, the dark blue one is chosen. This is because, according to the literature research, the transfer function should be approximately similar [1]. In addition, the obtained transfer function was accepted as correct since it should be approximately similar to the linear transfer function. In the following sections, calculations will be made using this transfer function. The transfer function of the nonlinear vehicle is as seen in Figure 4.5.

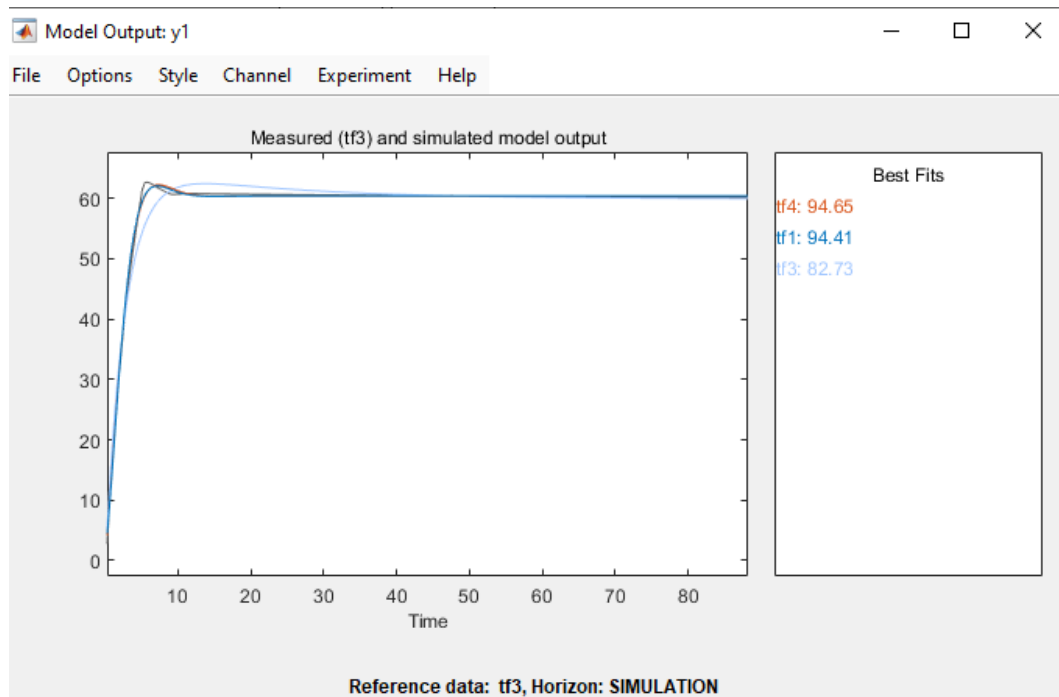


Figure 4.4: Estimated Results for Nonlinear Vehicle

```

From input "ul" to output "yl":
      0.397
-----
s^2 + 0.9471 s + 0.3943

Name: tfl
Continuous-time identified transfer function.

```

Figure 4.5: Estimated Transfer Function of Nonlinear Vehicle

4.2 Feedback Controller Design

This section describes the design of the feedback control structure. In cooperative adaptive and adaptive cruise control systems, a feedback control structure is required for the system to function smoothly. To maintain the desired positional difference between vehicles, the system continuously monitors this differential by taking the difference between the current position of its own vehicle and the position of the vehicle being followed. Therefore, the feedback control structure, as shown in Figure 4.6, has been employed. While using this structure, a PD (Proportional-Derivative) controller design has been implemented. With the PD controller, the system achieves the desired value with much less overshoot. This prevents the vehicle from accelerating more than necessary. Thus, by making the acceleration and deceleration of the vehicle smoother, a more comfortable driving experience is provided from the driver's perspective. The primary reason for choosing a PD controller in the design is the need for the system to operate very quickly during cruise; hence, the PD controller design has been implemented. The following equations have been used while obtaining the PD controller coefficients:

$$C_{fb,i}(s) = K_p + K_d s \quad (4.2)$$

$$G_i(s) = \frac{X_i(s)}{U(s)} = \frac{1}{s^2(\tau_i s + 1)} \quad (4.3)$$

$$H_i(s) = 1 + h_i s \quad (4.4)$$

In the derivation of in (4.2), $C_{fb,i}(s)$ represents the feedback controller, where K_p is the proportional coefficient of the feedback controller, and K_d denotes the derivative

coefficient of the feedback controller. The function $G_i(s)$ utilized in the derivation in (4.3) corresponds to the linear vehicle system, $X_i(s)$ indicates the position of the i-th vehicle, $U(s)$ is the controller input, and represents τ_i the uncertain time constant of the longitudinal vehicle dynamics. The term h_i in (4.4) specifies the following time.

When the controller design assumes $H_i(s) = 1$ the closed-loop transfer function of the system with feedback can be expressed as follows:

$$G_{CL}(s) = \frac{C_{fb,i}(s)G_i(s)H_i(s)}{1+C_{fb,i}(s)G_i(s)H_i(s)} \quad (4.5)$$

$$G_{CL}(s) = \frac{(K_p+K_d s)\left(\frac{1}{s^2(\tau_i s+1)}\right)}{1+(K_p+K_d s)\left(\frac{1}{s^2(\tau_i s+1)}\right)} \quad (4.6)$$

$$G_{CL}(s) = \frac{\frac{(K_p+K_d s)}{\tau_i s^3+s^2}}{1+\frac{(K_p+K_d s)}{\tau_i s^3+s^2}} \quad (4.7)$$

$$G_{CL}(s) = \frac{(K_p+K_d s)}{\tau_i s^3+s^2+K_d s+K_p} \quad (4.8)$$

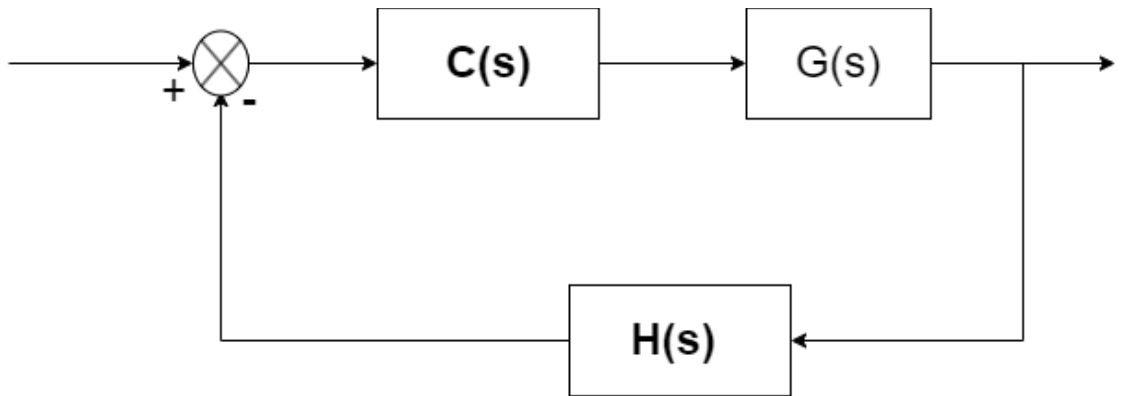


Figure 4.6: Close-loop Feedback Controller. In this figure, $C(s)$ is representing as a controller and $G(s)$ is plant of the vehicle. By sensors measure $H(s)$ as a feedback.

In the feedback controller shown in Figure 4.6, the input of the system is the speed of the vehicle in front. Feedback $H(s)$ represents the safe following time that the vehicle behind must leave between it and the vehicle in front. The speed information of the vehicle in front received from the sensor creates a distance in accordance with the 2

second rule (see Section 2.2.1.2). In the next section, the ACC system is explained in detail.

4.3 Adaptive Cruise Controller Design

When the simple block structure in Figure 4.6 for the adaptive cruise control design is examined, $G(s)$ is equal to the plant of the system,

$$G(s) = \frac{0.397}{s^2 + 0.9471s + 0.3943} \quad (4.9)$$

Since the two vehicle structures are homogeneous, two identical plants were used. First, the vehicle in front (Lead Car) is fed rapidly and the position information of the vehicle in front is transmitted to the sensor of the vehicle behind. This sensor can be rangefinder sensors, LIDAR sensors, RADAR sensors or cameras. Position information output is obtained by integrating the speed information of the vehicle in front. The speed information coming from the sensor enters the designed PD controller and the controller provides speed control of the vehicle in front. The controller output enters the following vehicle (referred to as Ego) behind. The ego vehicle outputs speed and position information is obtained by integrating this speed. The feedback structure collects speed information and position information to the sensor in (3.30). The collected information is transmitted to the sensors and given to the controller. This feedback structure is simply shown in Figure 4.8, and the more detailed Simulink structure is shown in Figure 4.9.

Two different methods were used for controller design. Among these methods, PD design provides a precise design with the root locus method. PD design details are described in Section 4.3.1. As another method, tuning was done with Genetic Algorithm. Tuning is not done according to a precise design data. By simply examining the desired state outputs, close values are made manually or by randomly (increased or decreased by certain multiple) changing the parameters. Details of the genetic algorithm are explained in Section 4.3.2.

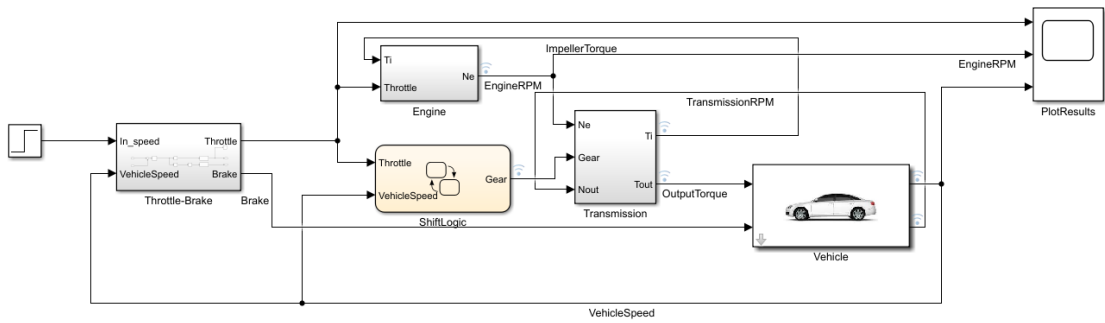


Figure 4.7: All of the Vehicle block diagram in MATLAB/Simulink.

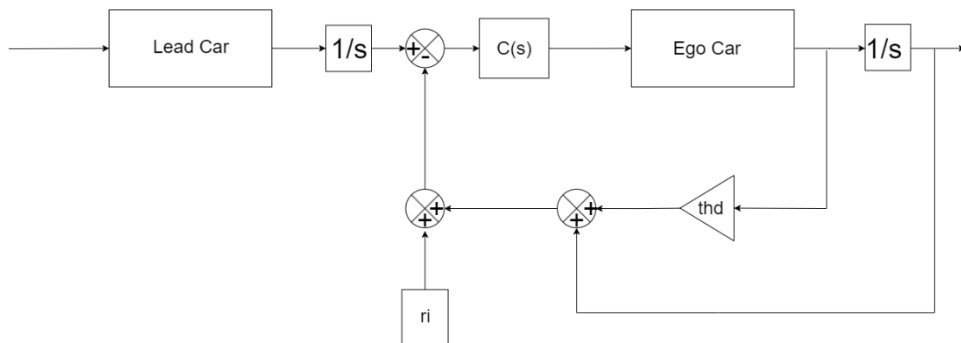


Figure 4.8: ACC basic block diagram structure.

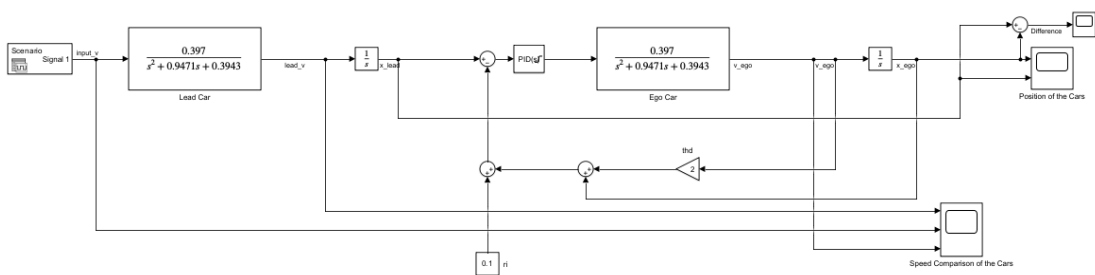


Figure 4.9: All of the ACC vehicle block diagram in MATLAB/Simulink.

4.3.1 ACC Controller Design with PD Controller

In this section, PD control design for ACC is done by hand calculations. The reason for using a PD controller is to shorten the response time to the error signal, to reduce oscillation and to provide smooth and stable control of the vehicle's speed and following distance settings. In order to design the PD controller, a simplified block diagram of the ACC model was first needed. Figure 4.10 shows the simplified block diagram obtained. Then the open-loop transfer function required for the root locus method described in the next section is obtained. Open-loop zero and poles are calculated.

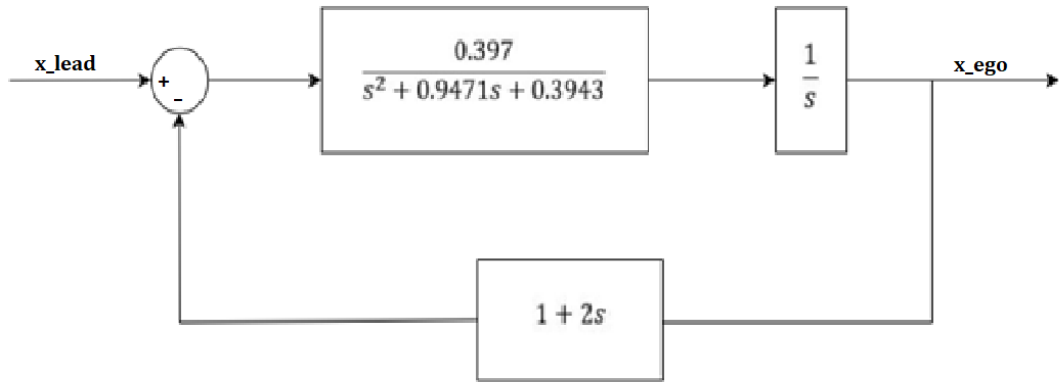


Figure 4.10: Simplified Block Diagram of the ACC Model

Open-Loop transfer function simplified vehicle model block diagram is,

$$OLTF = \frac{0.397(1+2s)}{s(s^2+0.9471s+0.3943)} \quad (4.10)$$

Open-loop poles are $p_1 = 0, p_{2,3} = -0.474 \pm j0.412$ and open loop zero is $z_1 = -0.5$.

4.3.1.1 Root Locus Properties

In this section, the characteristics of the root locus are mentioned in order to apply the root locus method that will be used when designing the ideal derivative compensator.

Angle and Magnitude Conditions: The explanations have been made considering the closed-loop transfer function of the negative feedback system shown in Figure 4.10. For ease of explanation, the transfer functions have been named and transfer function of the vehicle in (4.9).

$$G_I(s) = \frac{1}{s} \quad (4.11)$$

$$H(s) = 1 + 2s \quad (4.12)$$

Closed loop transfer function of the system,

$$\frac{x_{ego}}{x_{lead}} = \frac{G(s)G_I(s)}{1+G(s)G_I(s)H(s)} \quad (4.13)$$

The characteristic equation for this closed loop transfer function [14],

$$1 + G(s)G_I(s)H(s) = 0 \text{ or}$$

$$G(s)G_I(s)H(s) = -1 \quad (4.14)$$

Since $G(s)G_I(s)H(s)$ is a complex quantity, in (4.14) can be split into two equations by equating the angles and magnitudes of both sides respectively to obtain the following.

Angle conditions calculated as in below [14]

$$\angle G(s)G_I(s)H(s) = \pm 180^\circ(2k + 1) \quad (k = 0,1,2, \dots) \quad (4.15)$$

Magnitude conditions calculated as in below

$$|G(s)G_I(s)H(s)| = 1 \quad (4.16)$$

The values of s that satisfy both the angle and magnitude conditions are the roots of the characteristic equation, also known as the closed-loop poles. The root locus is the set of points in the complex plane that satisfy the angle condition alone. The roots of the characteristic equation (the closed-loop poles) for a specific gain value can be determined by the magnitude condition [14].

4.3.1.2 Design of an Ideal Derivative Compensator with Root Locus Techniques

In this section, the root locus technique is applied according to the open-loop transfer function obtained and the closed loop poles of the compensated system are determined on the root locus according to the desired damping ratio and settling time values. The damping ratio value was determined as 0.707 [1] and the settling time value was determined as 1.48 seconds. First, the angle θ_D that needs to be added so that the sum of the angles of the open loop poles and zeros of the original system at the desired

location of one of the dominant closed loop poles equals $\pm 180^\circ (2k+1)$ is in (4.15). The position of the added zero was then calculated using trigonometry methods.

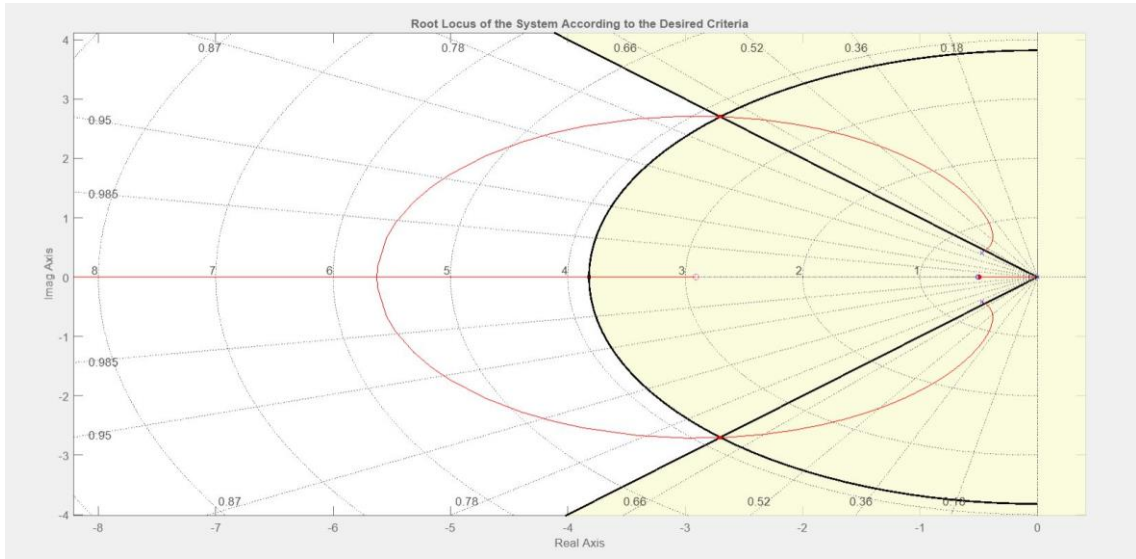


Figure 4.11: Root Locus of the System According to Specified Criteria [15]

According to the design criteria applied in Matlab Control System Designer app [15], $\zeta = 0.707$, $T_s = 1.48s$, $w_n = 3.82 \text{ rad/s}$, desired closed-loop poles are $-2.701 \pm j2.701$.

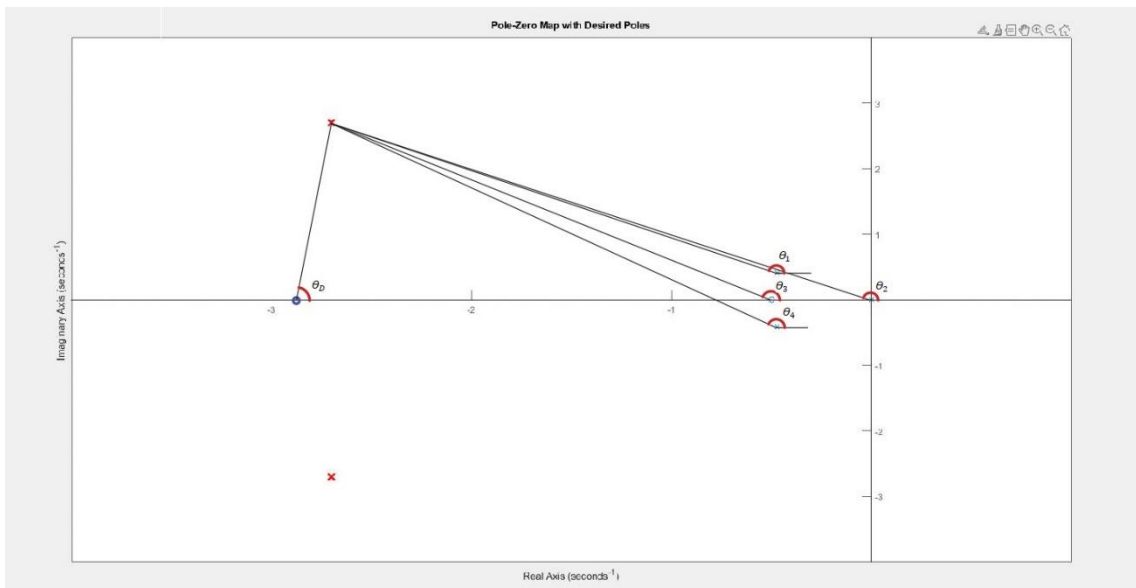


Figure 4.12: Diagram showing angle measurements from open loop poles and open loop zero to desired closed loop pole

In the following operations, the angles in Figure 4.12 were calculated and the alphas angle was found from the angle condition in (4.15).

$$\theta_1 = 180 - \tan^{-1} \frac{2.701-0.412}{2.701-0.474} = 134.2134377^\circ \quad (4.17)$$

$$\theta_2 = 180 - \tan^{-1} 1 = 135^\circ \quad (4.18)$$

$$\theta_3 = 180 - \tan^{-1} \frac{2.701}{2.701-0.5} = 129.1760188^\circ \quad (4.19)$$

$$\theta_4 = 180 - \tan^{-1} \frac{2.701+0.412}{2.701-0.474} = 125.5794411^\circ \quad (4.20)$$

Angle contribution of the ideal derivative compensator [14]

$$\theta_D + \theta_3 - \theta_4 - \theta_2 - \theta_1 = \pm 180^\circ (2k + 1) \quad (4.21)$$

Which is θ_D equal to 85.5377993° .

$z_d = 2.91$ was calculated in (4.22) with the help of trigonometry according to the angle found,

$$\tan(85.5377993^\circ) = \frac{2.701}{z_d - 2.701} \quad (4.22)$$

Finding the gain constant from the magnitude condition in (4.16), then

$$\text{Magnitude Condition : } 1 + \frac{0.397(1+2s)K_C(s+2.91)}{s(s^2+0.9471s+0.3943)} = 0 \quad (4.23)$$

$$K_C = \frac{-s(s^2+0.9471s+0.3943)}{0.397(s+2.91)(2s+1)} \quad (4.24)$$

$$K_C = \left| \frac{-s(s+0.474+j0.412)(s+0.474-j0.412)}{(s+2.91)(0.794s+0.397)} \right|_{s=-2.701+j2.701} \quad (4.25)$$

Which is equal to $K_C = 6.23$.

Thus, the Ideal Derivative compensator transfer function is found as follows,

$$G_{PD} = 6.23(s + 2.91) \quad (4.26)$$

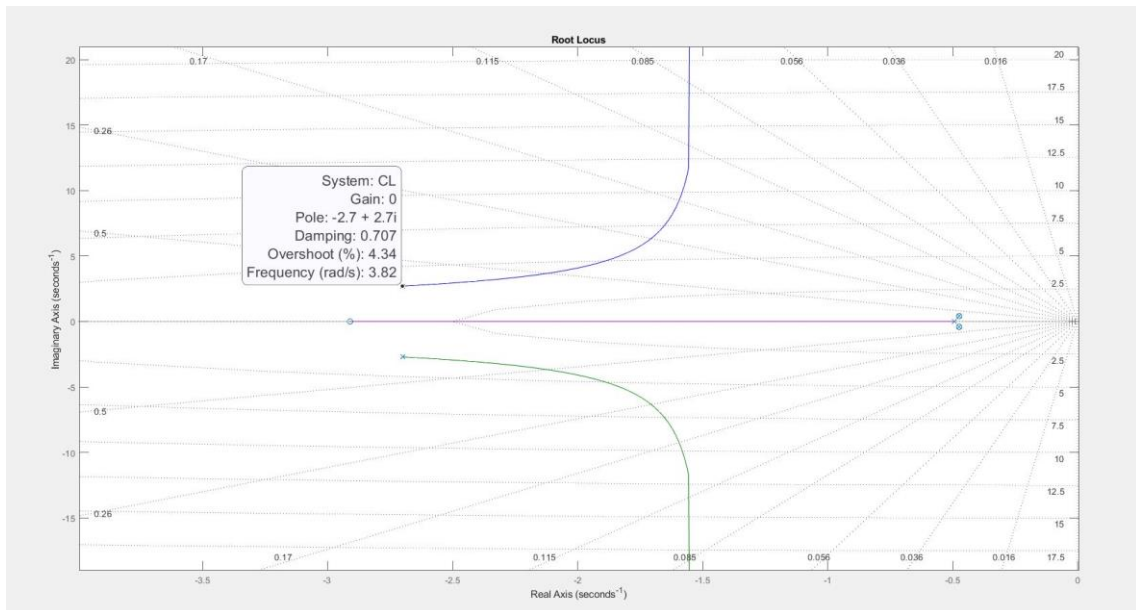


Figure 4.13: Root Locus of the Closed-Loop of the Compensated System

As you can see in Figure 4.13, the desired designing criteria were achieved with the ideal derivative compensator designed.

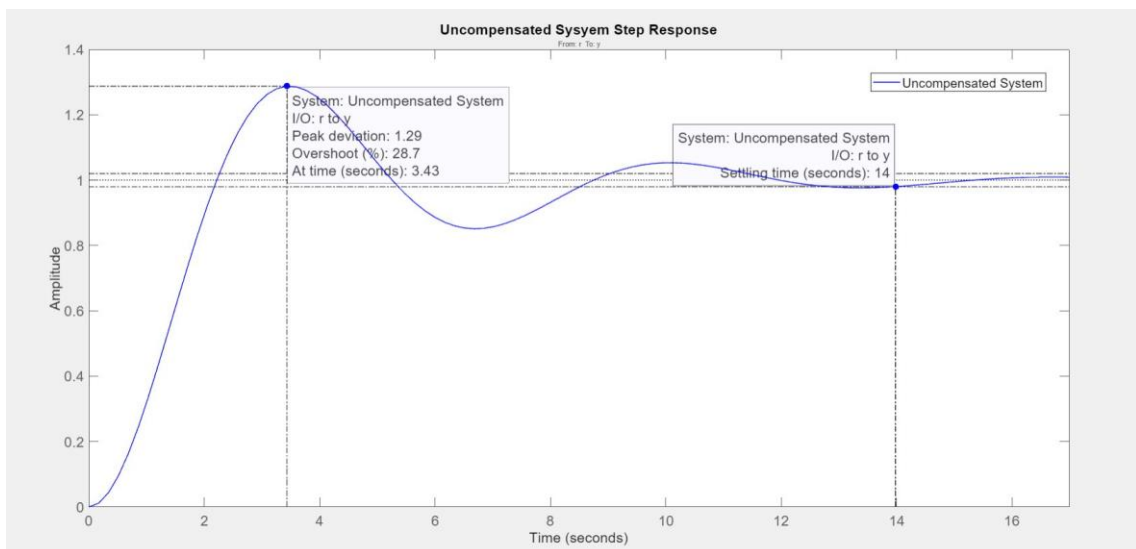


Figure 4.14: Step response of the uncompensated system displayed with the Matlab Sisotool Command [15]

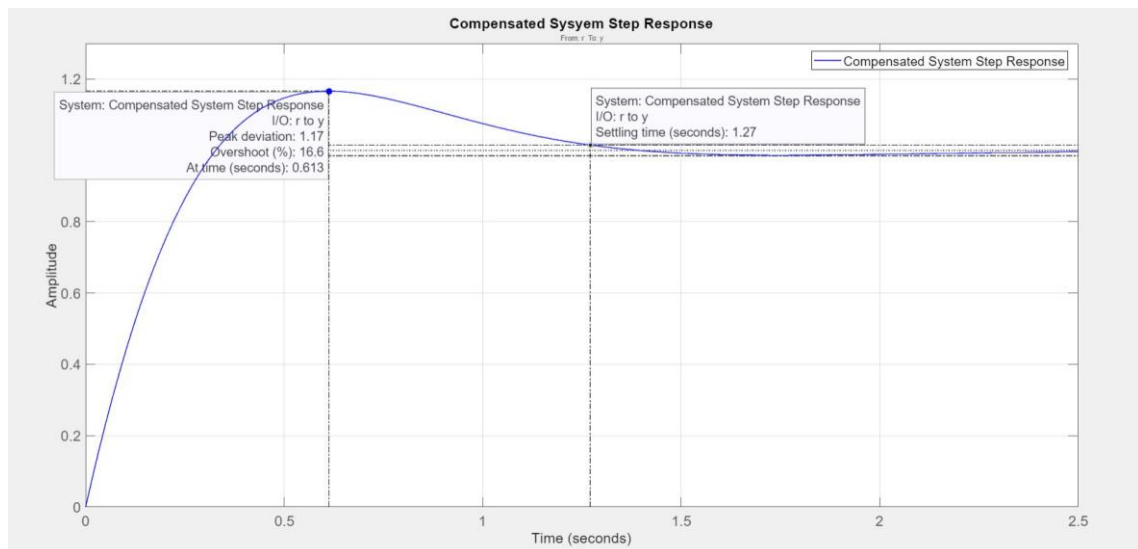


Figure 4.15: Step response of the compensated system displayed with the Matlab Sisotool Command [15]

The step responses seen in Figures 4.14 and 4.15 show that the ideal derivative compensator designed with the root locus technique significantly improves the dynamics of the system. It can be seen that the compensated system has lower overshoot and faster settling time.

The small differences between the step response of the compensated system and the values obtained from mathematical calculations can be attributed to the second-order approximation made when analyzing the system's step response and the error margins used by the MATLAB Sisotool command in finding these values.

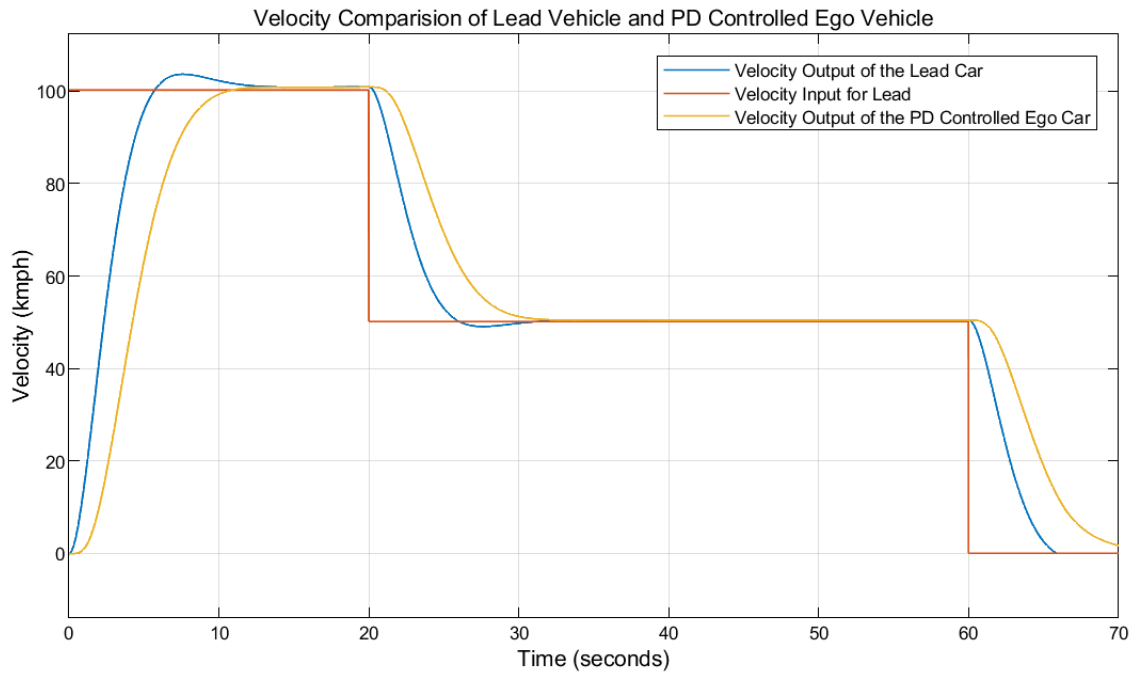


Figure 4.16: Velocity Comparison of Lead Vehicle and PD Controlled Ego Vehicle

Figure 4.16 shows the input speed signal given to the lead vehicle and the speed of the lead vehicle output and the ego vehicle output. The red line is shows the given for the lead vehicle input speed signal, blue line is shows the velocity output of the lead vehicle and yellow line is shows the velocity output of the ego vehicle. Vehicle speeds are given in kilometers/hour over a 70-second period.

While the lead car gives a speed output depending on the vehicle dynamics in line with the input speed signal, the ego car reveals the performance of the ACC system designed to follow the lead car.

Figure 4.16 shows that factors such as the smoother acceleration and deceleration transitions of the Ego vehicle and the reaction delay illustrate the ACC model's effort to maintain a safe following distance and prevent sudden braking and throttle changes, thereby enhancing passenger comfort and safety.

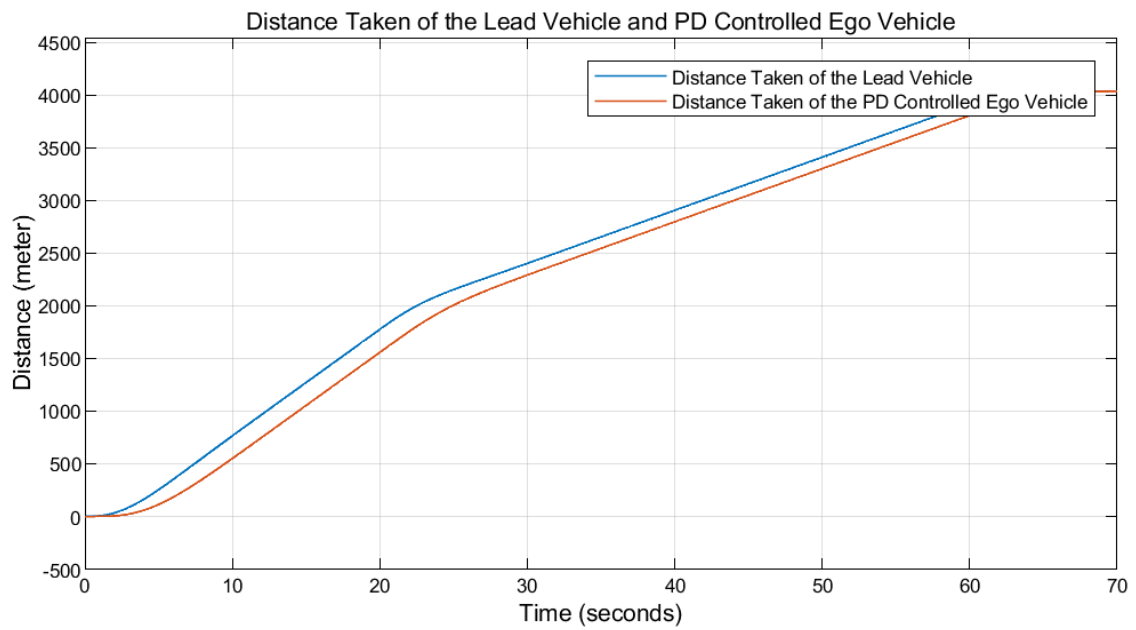


Figure 4.17: Comparison of the taken distance of the lead vehicle and PD controlled ego vehicle

Figure 4.17 shows the distances traveled by the lead vehicle and the ego vehicle over time. The blue line shows the distance traveled by the lead car, while the red line shows the distance traveled by the ego car. The distance traveled is expressed in meters, and the time is expressed in seconds. The graphic covers a period of 70 seconds.

Since the lead car travels more distance than the ego car during acceleration and deceleration, the desired distance difference changes minimally and, in general, it appears that the ego car follows the lead car effectively.

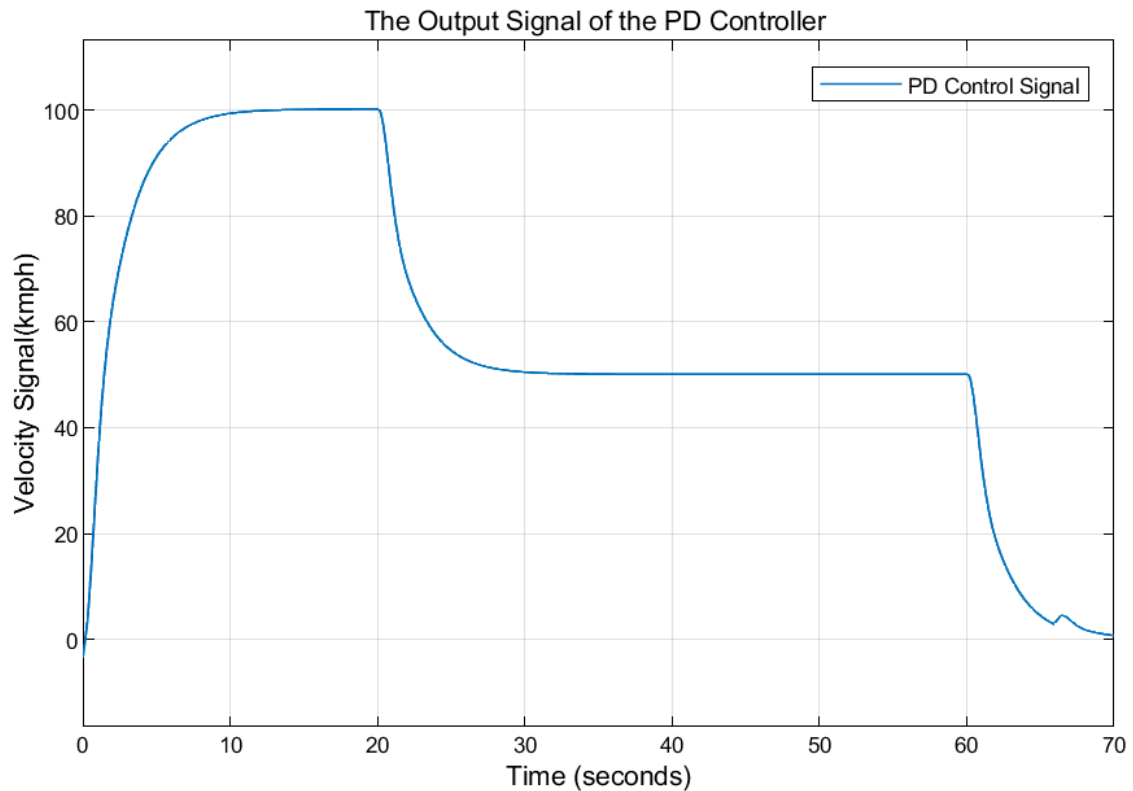


Figure 4.18: The output signal of the PD controller designed using the root locus technique.

Figure 4.18 shows the performance of the output signal of the PD controller designed using the root locus technique. The speed signal is shown in kilometer per hour and the time in seconds, and the signal covers a period of 70 seconds.

The PD control signal has successfully accomplished the task of increasing the speed signal steadily and quickly, keeping it constant at certain speed levels, and gradually decreasing it. It can be seen that the designed PD controller manages the speed signal effectively.

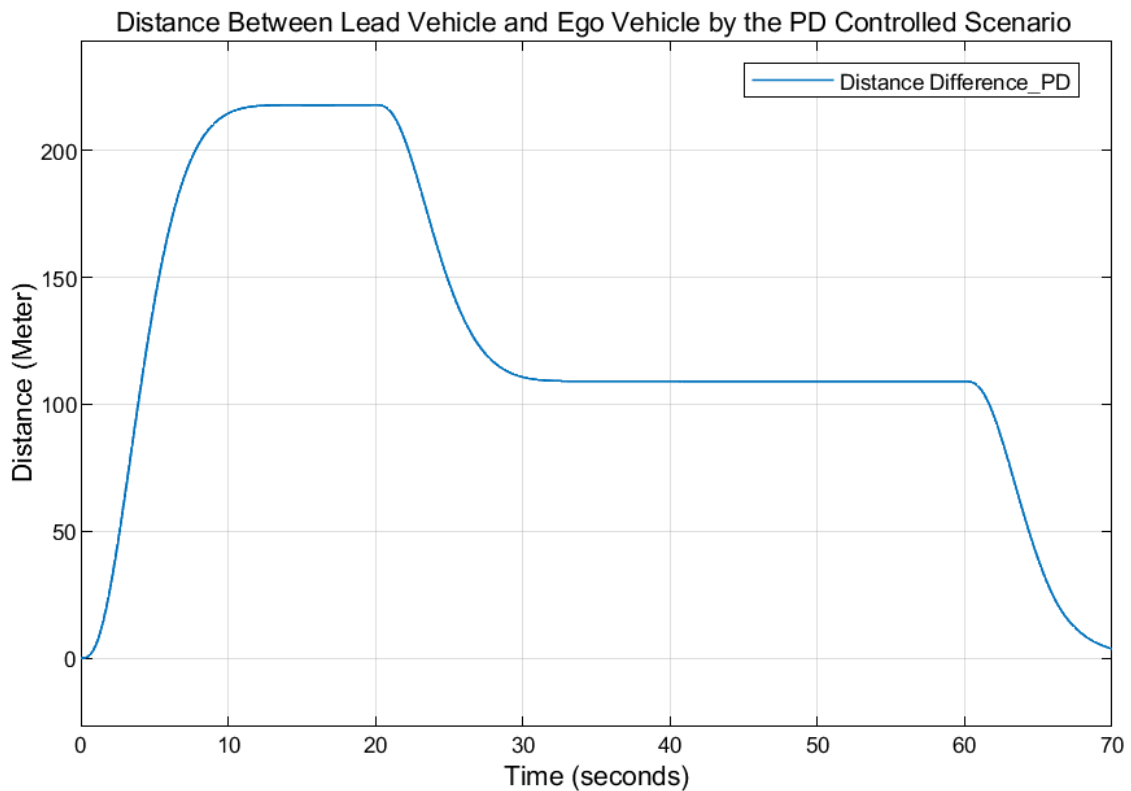


Figure 4.19: Distance Between Lead Vehicle and Ego Vehicle by the PD Controlled Scenario

Figure 4.19 shows the distance difference between two vehicles. As seen in Figure 4.9, since the constant time value is 2 second, twice the current velocity provides the desired distance between vehicles. It was observed that the velocity of the vehicles increased until the 10th second and the distance between the vehicles increased with increasing velocities. When the vehicle velocities equalized after the 10th second, the distance control required for the current velocity value was achieved, and when the velocity of the vehicles started to decrease after the 20th second, the desired distance value between them decreased along with the decreasing velocity. Later, when the velocity were equalized again, distance stability was achieved and the distance between the vehicles continued to decrease until the both vehicles came to a halt.

4.3.2 ACC Controller Tuning with Genetic Algorithm

In this subsection, Adaptive Cruise Controller has been tuned with Genetic Algorithm. As mentioned before, elite individuals are selected according to the lowest cost function

output in the generation and transferred to the next generation. The mentioned cost function comes from the LQR calculation

$$J = \int (x^T \cdot Q \cdot x + u^T \cdot R \cdot u) dt \quad (4.27)$$

Equation 4.28 will be used, similar to the theoretically used LQR and cost calculation

$$J = \int_0^T (Q \cdot e(t)^2 + R \cdot u(t)^2) dt \quad (4.28)$$

$e(t)$ is the error function, that is, the difference between the desired output (usually a step function) and the actual system output $y(t)$. $e(t) = 1 - y(t)$. $u(t)$ is the control input, i.e. the signal applied by the controller to the system input. The weights Q and R represent the costs of error and control input, respectively. Q determines how much "penalty" to give for error, and R determines how much "penalty" to give for control effort.

In order to use this function more flexibly in MATLAB and to ensure convergence of the integral calculation, the cost function J is calculated in discrete time

$$J = \Delta t \sum_{k=0}^N (Q \cdot (1 - y(k))^2 + R \cdot u(k)^2) \quad (4.29)$$

Δt represents the time interval of the simulation steps. N is the total number of time steps, which depends on the length of the t vector. $y(k)$ and $u(k)$ are the system output and control input values at time step k .

If the J value is too high or too low, it may cause realistic problems in the system. If the J value is too high, it will cause excessive energy costs and inefficient operation of the system. For this, the constraints of the system must be determined and dynamically realistic tests are needed. Although the car constraints used in this thesis are not clear, the outputs will be discussed according to the lowest cost function among the data used.

4.3.2.1 Genetic Algorithm Implementation for PID Tune with MATLAB

In this section, genetic algorithm optimization using MATLAB will be discussed. MATLAB can be used when performing genetic algorithm optimization. For this, it is necessary to use the Global Optimization Toolbox [16]. The "ga()" function found here will optimize the system with the genetic algorithm.

When defining the function, it should be defined within the function as `ga(fitnessfcn,nvars,A,b,Aeq,beq,lb,ub,nonlcon,options)` respectively. The parameters inside the function are

fitnessfcn: The fitness function, which is the function to be minimized by the genetic algorithm. This function should take a vector (representing an individual in the population) as input and return a scalar fitness value.

nvars: The number of variables in the function, which corresponds to the number of elements in the vector that the fitness function accepts.

A, b: These are matrices used to define linear inequality constraints ($A*x \leq b$).

Aeq, beq: These are matrices used to define linear equality constraints ($Aeq*x = beq$).

lb, ub: Vectors defining the lower and upper bounds on the variables. These limit the search space for each variable.

nonlcon: A function handle for nonlinear constraints. This function should return two vectors, one for nonlinear inequality constraints and another for nonlinear equality constraints.

options: A structure that specifies options used by the genetic algorithm, such as population size, maximum number of generations, crossover and mutation functions, selection strategy, and so on.

For the feedback controlled system mentioned in the thesis, "dt" represents the sampling time, "PopSize" represents the population size, "MaxGenerations" represents the maximum number of generations, "tf" represents the transfer function in Laplace s, "G" represents $G(s)$.

```

dt=0.001; %sampling time
PopSize=25; %population size
MaxGenerations=10; %maximum generation
s = tf('s');
G= 0.397/(s*(s^2+0.9471*s+0.3943)) %nonlinear transfer function of vehicle
options = optimoptions(@ga, 'PopulationSize', PopSize, 'MaxGenerations',...
MaxGenerations); %GA function option
[x,fval] = ga(@(K)pidtest(G,dt,K),3,-eye(3),zeros(3,1))%GA function to
%estimate PID paramters

```

Figure 4.20: Code for the define the ACC system and Genetic algorithm function [17]

As seen in the code to calculate the cost function and find the PID parameters in Figure 4.20 above, x is defined for the PID and $fval$ is defined for the cost function. The internal structure of the `pidtest()` function is shown in Figure 4.21 below.

```

function J = pidtest(G,dt,parms)
    s = tf('s');
    K = parms(1) + parms(2)/s + parms(3)*s/(1+0.001*s); %Defining PID
%parameters as Kp+Kd.s+Kp/s
    Loop = series(K,G); % define PID controller and plant in series
%structure
    ClosedLoop = feedback(Loop,1+2*s); %for create our controlled loop as
%a feedback
    t = 0:dt:20; %time boundary initialize and sampling time as dt
    [y,t] = step(ClosedLoop,t); %step response for CLtf
    %H=1+2*s defined as feedback block H(s)
    CTRLtf = K/(1+K*G*(1+2*s)); %for define our controlled transfer
%function K/(1+KGH)
    u = lsim(CTRLtf,1-y,t); % u represents control input signal
%(1-y) represents error signal and lsim is simulate for the system with
time response

    Q = 1; %define Q value
    R = 0.001; %define R value
    J = dt*sum(Q*(1-y(:)).^2+R*u(:).^2) %calculates cost function
%(see eq 4.29)
%plotting settings for popping-figures
    [y,t] = step(ClosedLoop,t);
    plot(t,y,'LineWidth',2,'color','b')
    set(gca, 'color','k','color','w', 'color','w')
    set(gcf, 'color','w')
    grid on
    drawnow
end

```

Figure 4.21: Code for pidtest function for estimate PID parameters as P for $\text{parms}(1)$, I for $\text{parms}(2)$ and D for $\text{parms}(3)$ [17]

For the MATLAB script, it calculates the performance index J using the Quadratic Cost Function, which is common in control system optimization. This determines the weighting factor (Q) for the squared error term in the cost function. In control theory, Q

typically penalizes deviations from the desired output (tracking error). This sets the weighting factor R for the control effort term in the cost function. Smaller the R value means less settle time in control effort and allows for more aggressive control actions. This calculates the cost function J , which represents the performance of the control system. The formula can be explained down as follows

$Q*(1-y(:)).^2$: This term calculates the square of the error between the desired output (which is 1, representing a unit step input) and the actual output y . The weighting factor Q scales this error.

$R*u().^2$: This term calculates the square of the control effort (u) with the weight factor R .

$\text{sum}()$: This sums these quantities across all time steps.

$\text{dt}*$: Multiplying by dt (time step size) turns the sum into an integral that represents the total cost over a given time horizon.

While tuning the system with GA, Q and R parameters were determined, and numbers were given to obtain the most optimal lowest cost value used. Different scenarios were then tried to determine the best parameter range. When determining these scenarios, $Q=1$ was initially considered as $R=0.001$. 5 different scenarios are defined in the table 4.1 below. In the conclusion section, the outcomes of these scenarios will be evaluated.

Table 4.1: Scenarios for tuning PID parameters

Scenario	Q	R	J
1	1	0.001	1.3321
2	1	0.01	1.6782
3	1	1	3.2679
4	10	0.001	11.4173
5	100	0.001	105.2391

When the scenarios are analyzed in order, some criteria are needed. In order to find the best result, the low cost function J should be optimal, the distance between the vehicles should be optimal, especially the system should not be unstable, the vehicle behind should not get in front of the vehicle in front (in this case, the system is not working) and the speed response should not oscillate in steady-state velocity. System outputs were taken according to Figure 4.9.

To simply calculate the optimal distance between vehicles, it should be the safe following distance mentioned in Section 2.2.1.2. That is, if both vehicles are cruising at 100 kmph, the distance between them in steady-state should be $100 \text{ kmph} \times 2 \text{ seconds} = 200 \text{ meters}$.

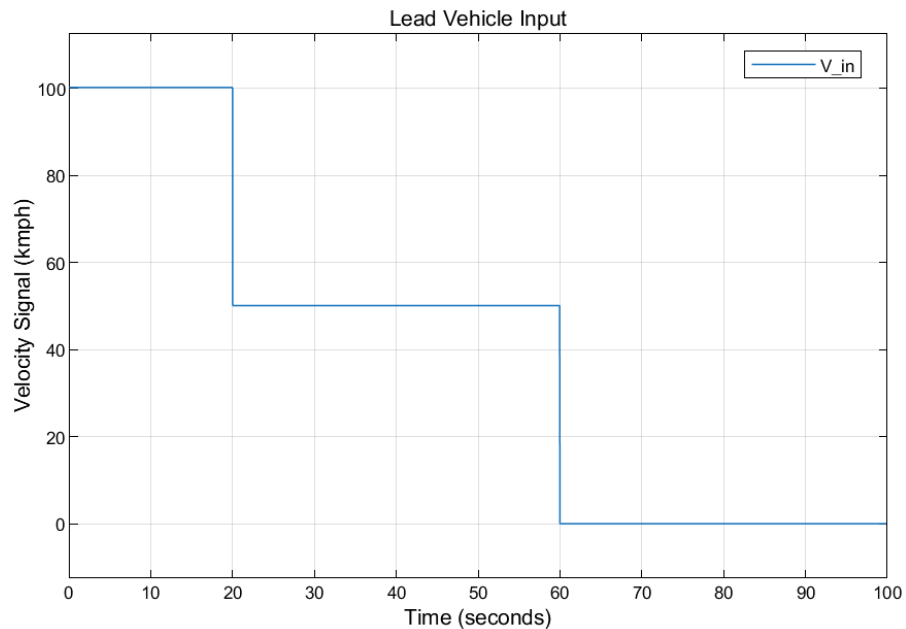


Figure 4.22: Velocity input of the vehicle in lead.

A scenario has been created for the vehicle in lead. According to the scenario, the vehicle in lead travels at a speed of 100 kmph between 0-20 seconds and at 50 kmph between 20-60 seconds as seen in the Figure 4.22. Also can be seen of the distance taken (4.4 km) of the lead car in Figure 4.24.

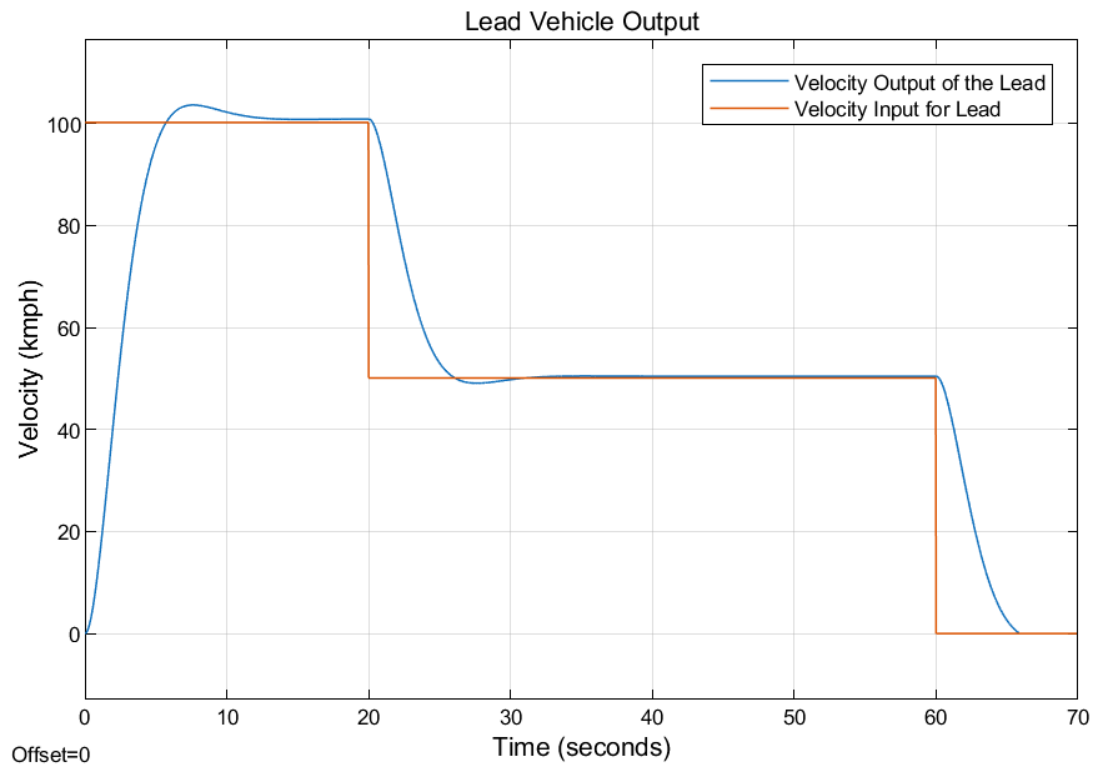


Figure 4.23: Velocity output of the lead vehicle.

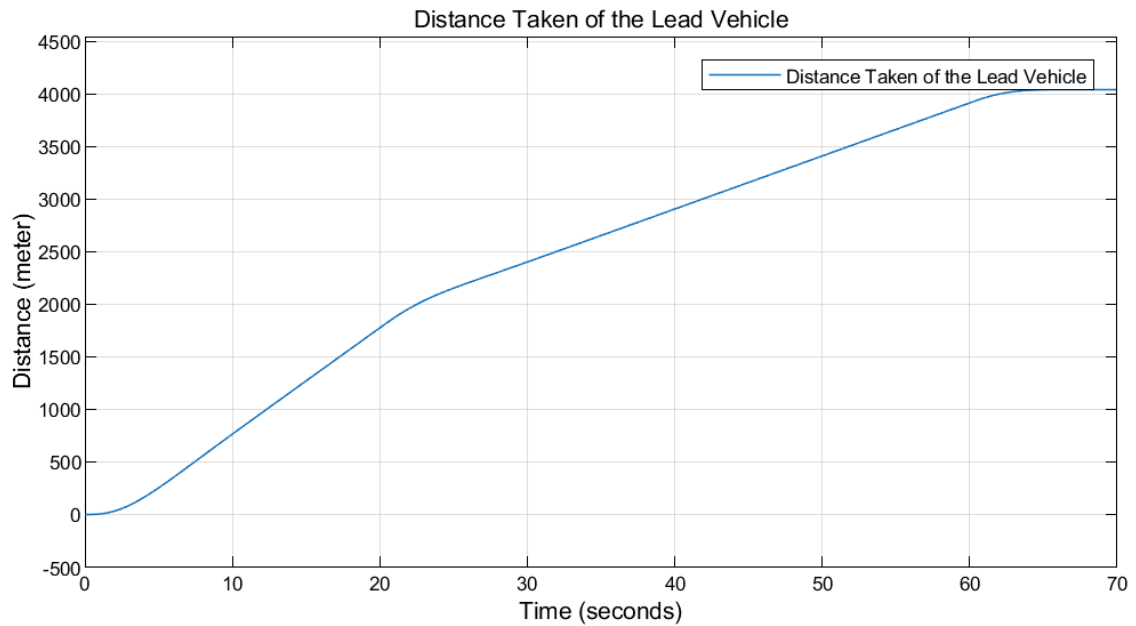


Figure 4.24: Distance taken of the lead vehicle.

After this the ACC system that done before is expected to follow the vehicle in front. Estimated Q and R values for genetic algorithm outputs are given in Table 4.2. Cost (J) values and PID parameters for these scenarios are given in the table below.

Table 4.2: Tuned PID values and cost (J) values according to different scenarios.

Scenario	Q	R	J	Kp	Ki	Kd
1	1	0.001	1.3321	6.9752	0	0.1199
2	1	0.01	1.6782	2.9065	0	0.0279
3	1	1	3.2679	0.5531	0.0046	0.0013
4	10	0.001	11.4173	16.1603	1.5273	0.388
5	100	0.001	105.2391	36.6277	11.5526	0.9325

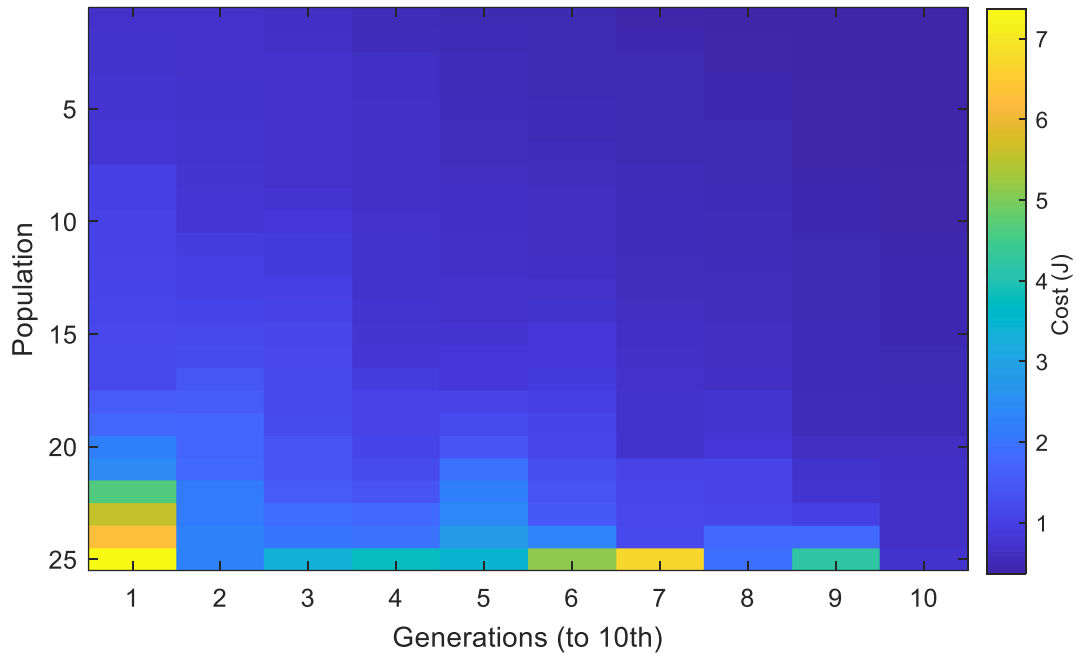


Figure 4.25: Genetic warmth map output of the genetic algorithm and relation with cost function J by the scenario 1.

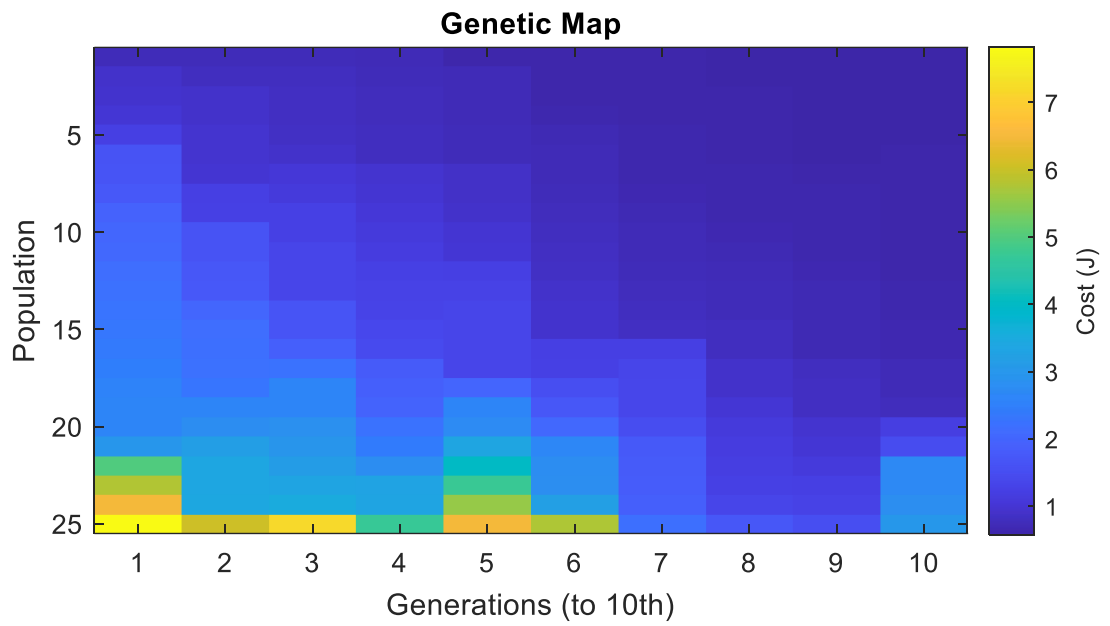


Figure 4.26: Genetic warmth map output of the genetic algorithm and relation with cost function J by the scenario 2.

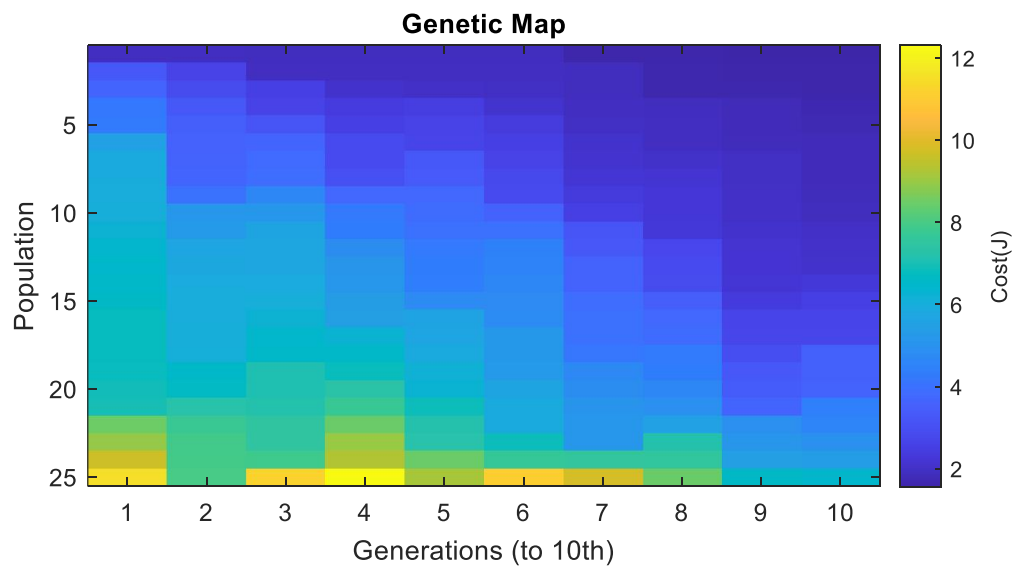


Figure 4.27: Genetic warmth map output of the genetic algorithm and relation with cost function J by the scenario 3.

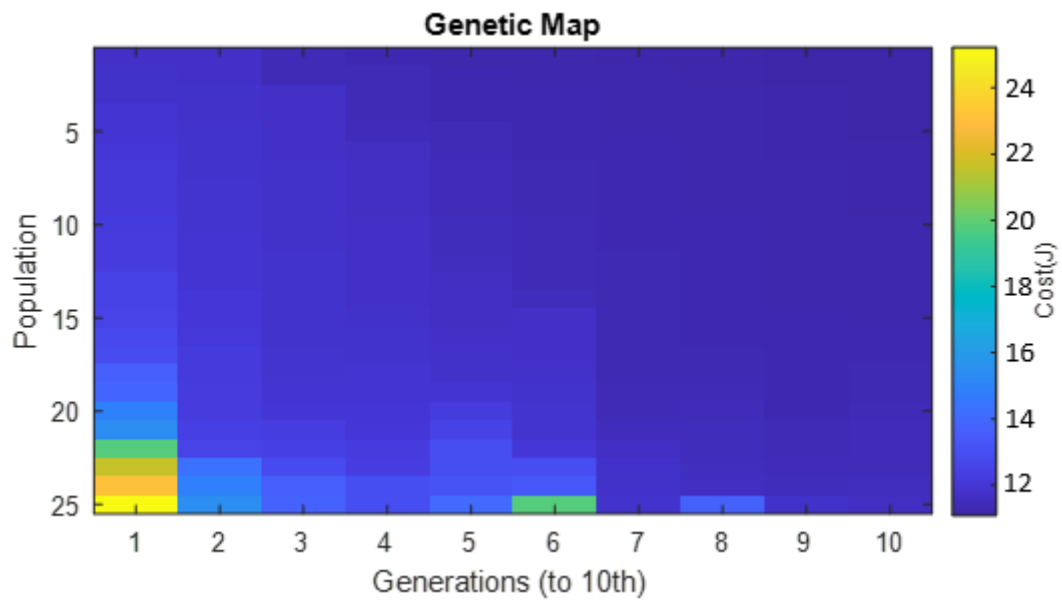


Figure 4.28: Genetic warmth map output of the genetic algorithm and relation with cost function J by the scenario 4.

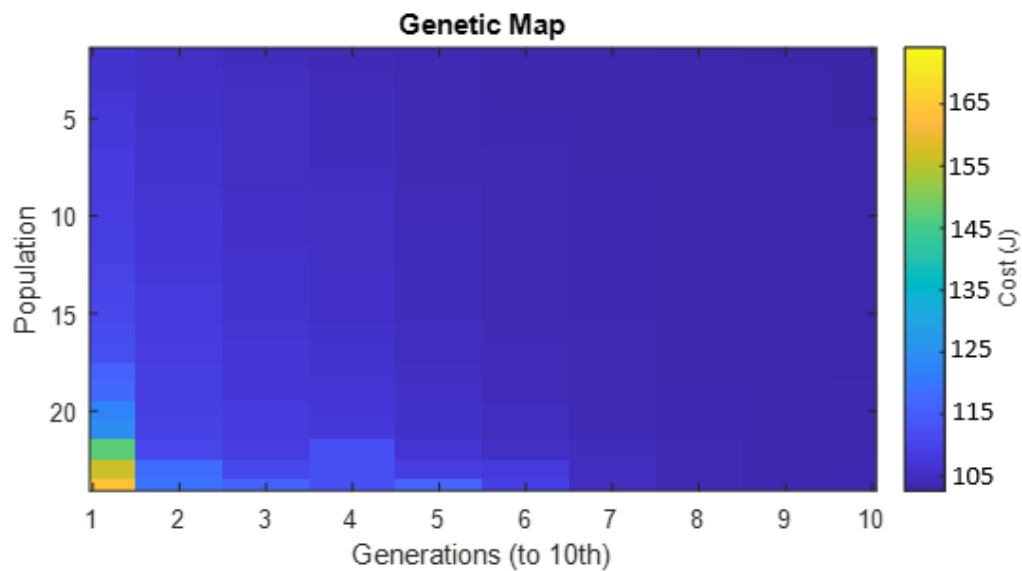


Figure 4.29: Genetic warmth map output of the genetic algorithm and relation with cost function J by the scenario 5.

The figures above are the outputs of the scenarios seen in Table 4.2. These outputs show the population-generation transmission of the genetic algorithm and the selection of elite individuals (elitism). Elite individuals are the result of the cost function. According

to the warmth map, warm colors indicate a high cost function. Cold colors represent low cost. There is a clearly visible temperature difference between the first generation and the last generation. The algorithm stops the prediction when it reaches the specified generation-population number. It selects the healthiest, that is the lowest cost number of the 10th generation and gives it as output (fva1 represents the final output in Figure 4.20. When comparing the scenarios, data with the low cost function was selected. Then the application of the estimated PID data is shown.

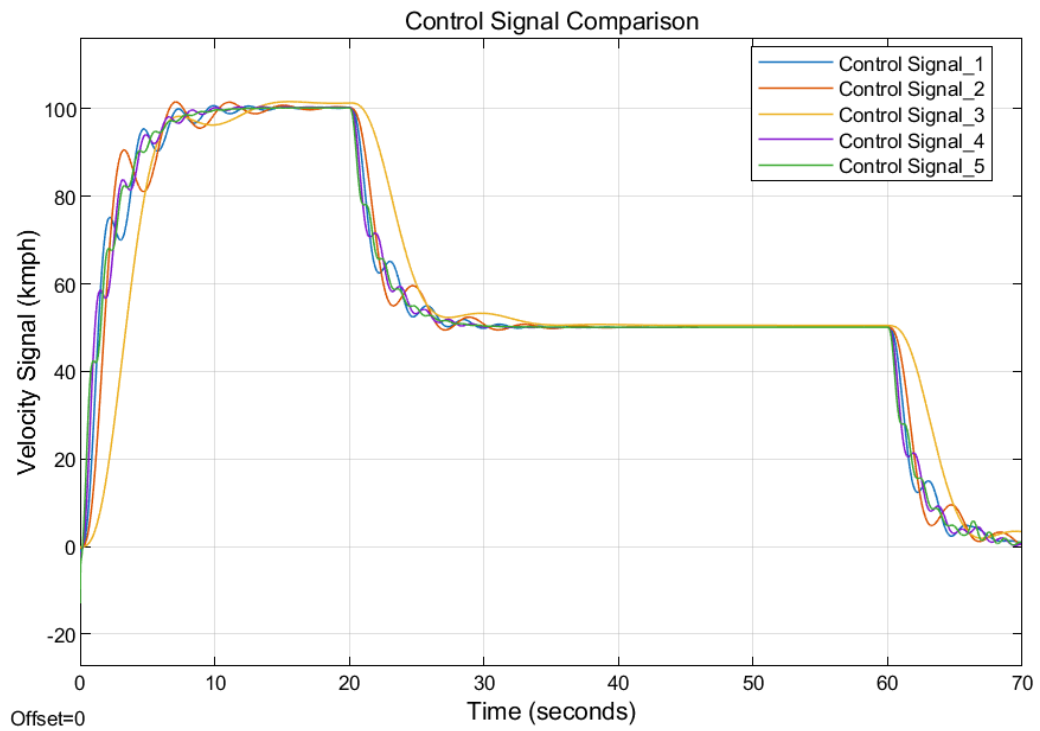


Figure 4.30: Comparison of the output signals PID tuned with genetic algorithm.

When the control signal outputs are examined according to the scenarios, scenario 1 is represented for Control Signal_1, scenario 2 for Control Signal_2, scenario 3 for Control Signal_3, scenario 4 for Control Signal_4 and scenario 5 for Control Signal_5. The signals appear to oscillate. These signals should not make the system unstable. When other outputs are examined (for example, velocity output), it is seen that it does not disrupt the vehicle's norms and does not create oscillations. According to these signals, it may be appropriate to choose the scenario with the least oscillation. According to these scenarios, the least oscillation is seen in scenario 3, but cannot make the choice right away.

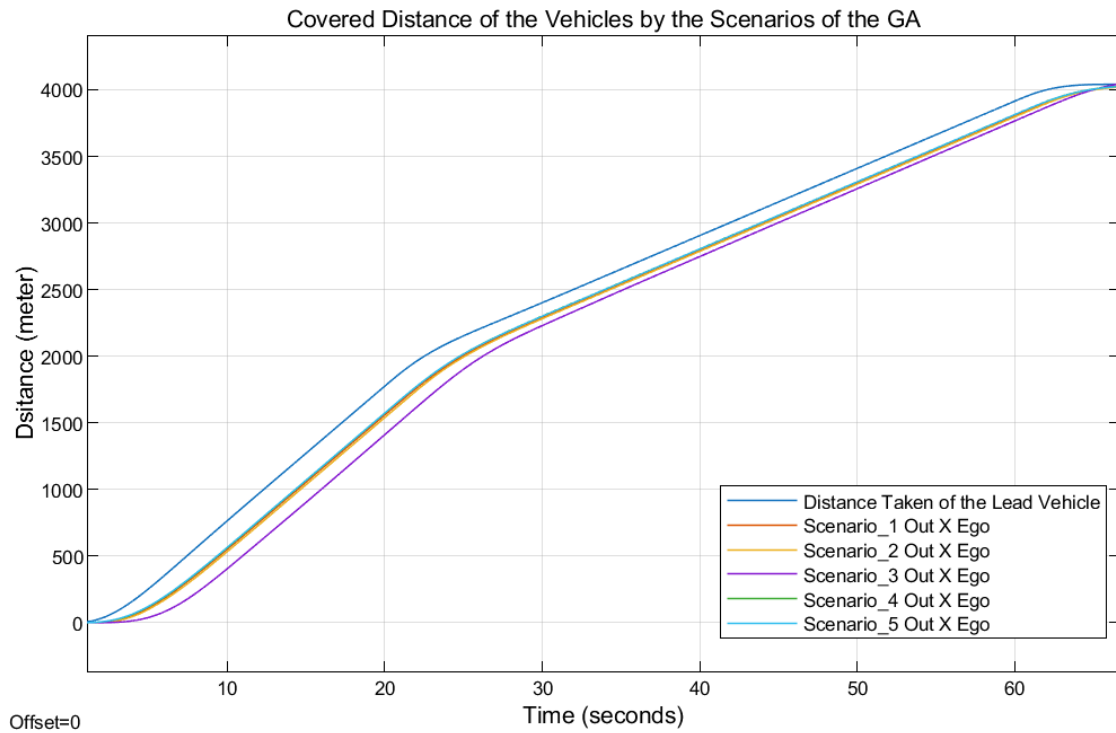


Figure 4.31: Covered distance of the vehicles by the scenarios of the Genetic Algorithm estimated PID tuning.

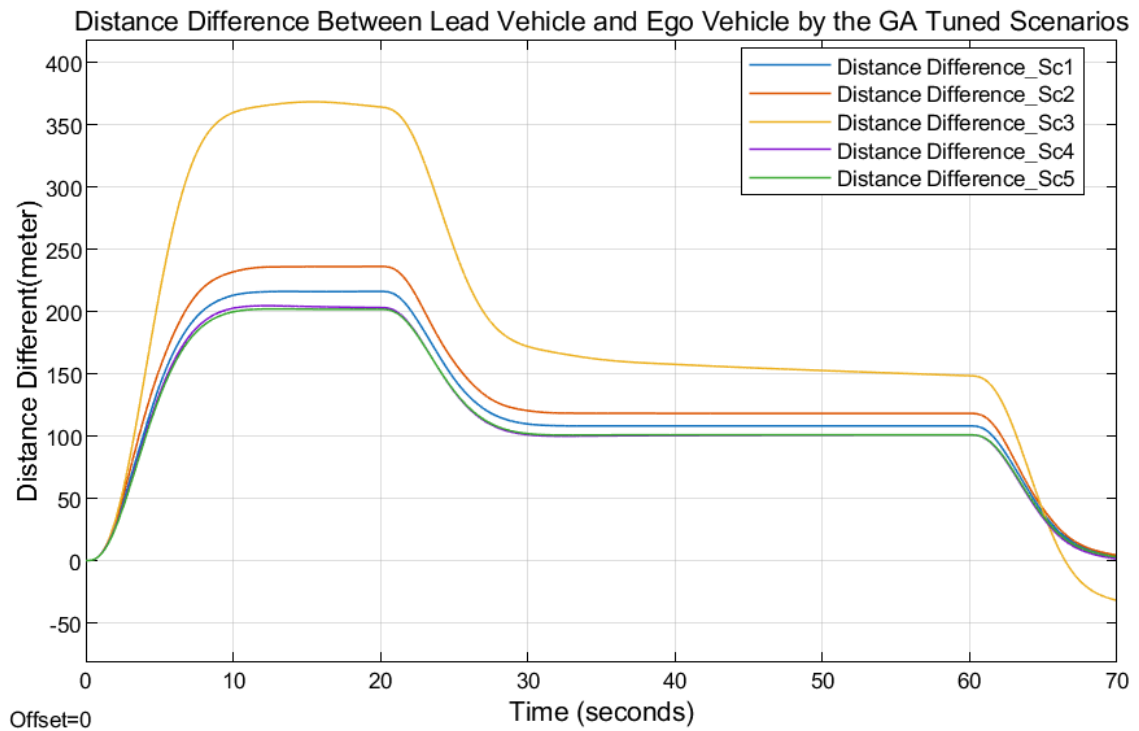


Figure 4.32: Distance difference between the lead and ego vehicles.

Looking at the distance output of the system, the leading vehicle was not overtaken in any scenario. However, for simple calculations, the mentioned safe distance should not be exceeded or to determine the most perfect scenario, the following distance rule

mentioned in Section 2.2.1 should be followed. In other words, when vehicles are traveling at 100 kmph, the distance between them should not be less than 200 meters. As seen in Figure 4.32, no scenario exceeds this value, but in scenario 3, there is an unnecessary distance difference (~360 meters) as seen at the 15th second.

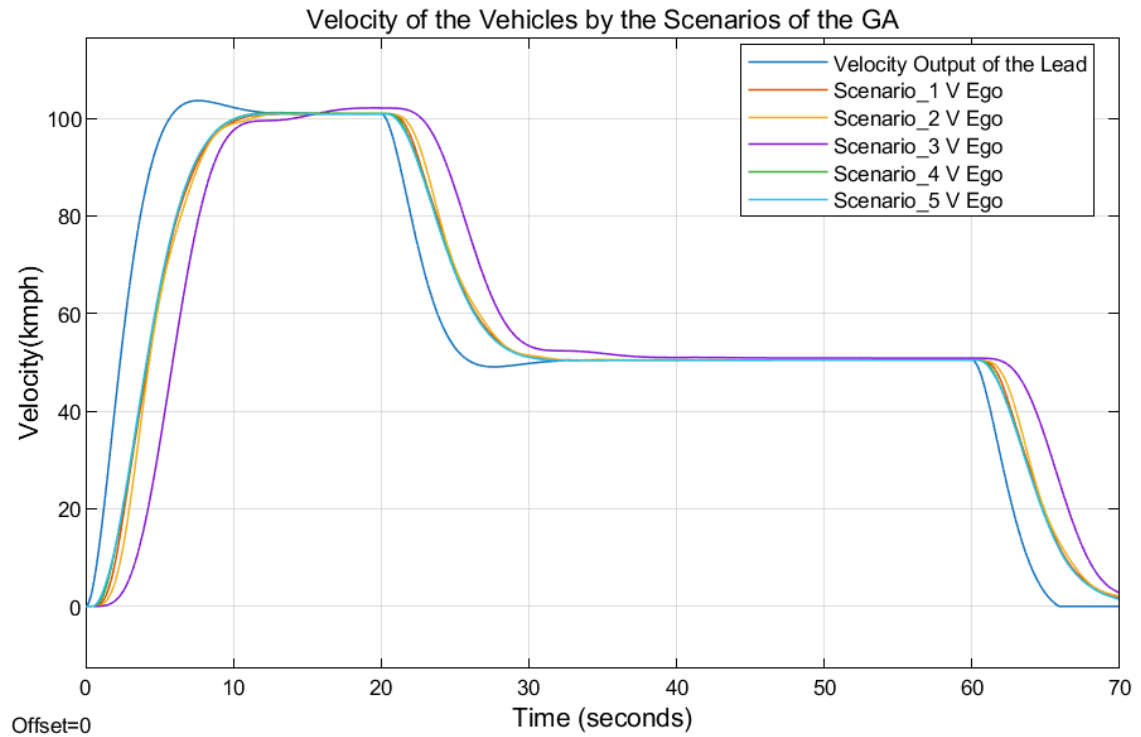


Figure 4.33: Velocity comparison of the vehicles by the scenarios.

As seen in the ACC velocity outputs, the velocity output for scenario 3 accelerated further than the lead vehicle traveling at 100 kmph in 15-20 seconds and could not maintain the distance behind it. Thus, scenario 3 is absolutely unusable and an incorrect guess. However, when the step response was examined, it was seen that scenarios 1 and 2 also disrupted the system and created oscillations. When the step response of scenarios 4 and 5, which are the best choices, are examined according to the open loop, results are as in Figures 4.34 and 4.35.

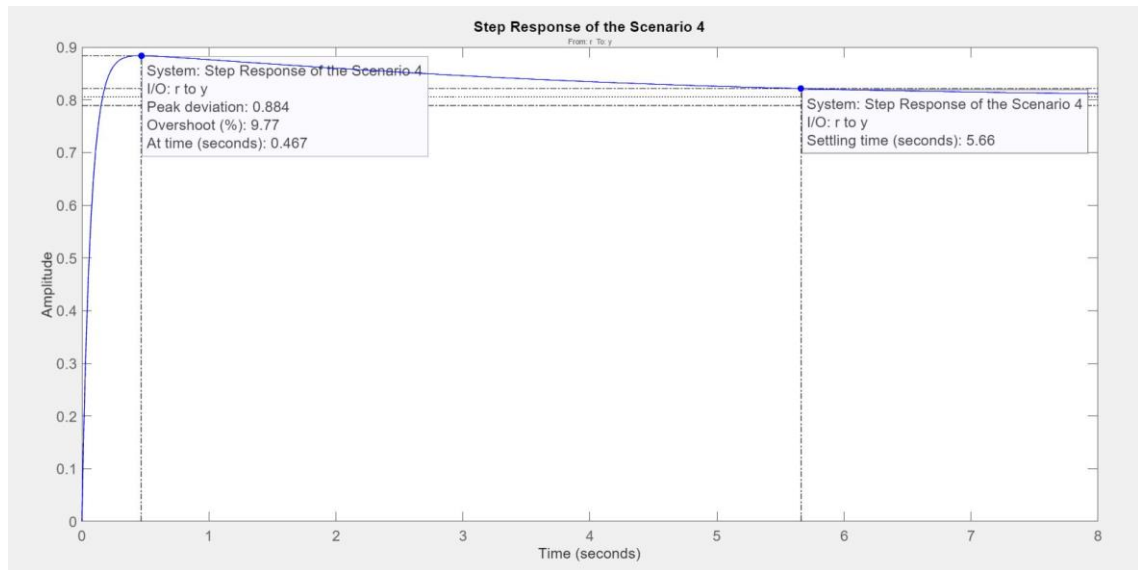


Figure 4.34: Step response of the scenario 4.

According to the output of scenario 4 seen in the Figure 4.34 above in (parameters can be examined in Table 4.2), the system constantly gives steady state errors. The system gives a steady state error of $1 - 0.8 = 0.2$ according to the step response. The system settles in 5.6 seconds. According to this result, if the steady state error is tuned again by increasing the I-integral, the error will be eliminated. However, since the system is very slow, using scenario 4 will be not appropriate.

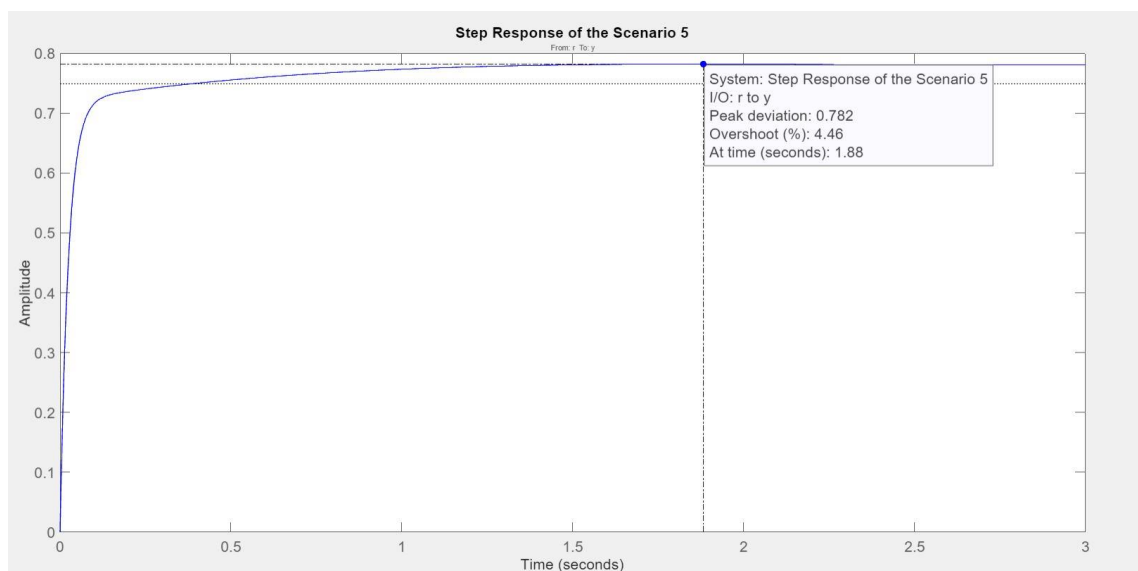


Figure 4.35: Step response of the scenario 5

According to the output of scenario 5 seen in the Figure 4.35 above (parameters can be examined in Table 4.2), the system constantly gives steady state errors. The system gives a steady state error of $1 - 0.8 = 0.2$ according to the step response. The system settles in 1.88 seconds. According to this result, if the steady state error is tuned again by increasing the I-integral, the error will be eliminated. When the necessary tuning is done, the system will settle faster and the steady state error will be eliminated. It would be appropriate to use this system. For the comparisons that follow in the thesis, the performance of the genetic algorithm function will be examined and the comparisons will be discussed without any further intervention.

4.4 Comparison of the Designed PD Controller and GA Tuned Controller

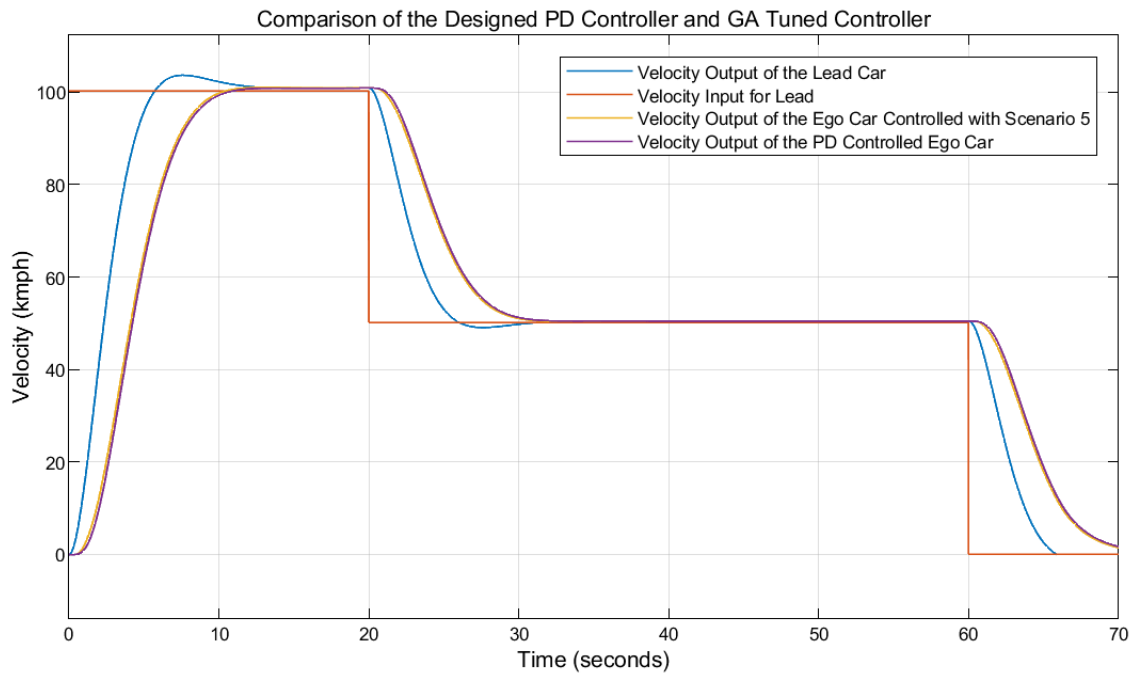


Figure 4.36: Comparison of the Designed PD Controller and GA Tuned Controller

In Figure 4.36 compares the performance of a PD controller designed using the root locus technique and a Genetic Algorithm (GA) tuned controller in speed control of the ego vehicle. The GA tuned controller exhibits improved response speed and control precision, allowing the ego vehicle to more accurately follow the speed changes of the vehicle in front with less delay. In contrast, the PD controller provides smoother control but causes delays in the ego vehicle's response to speed changes.

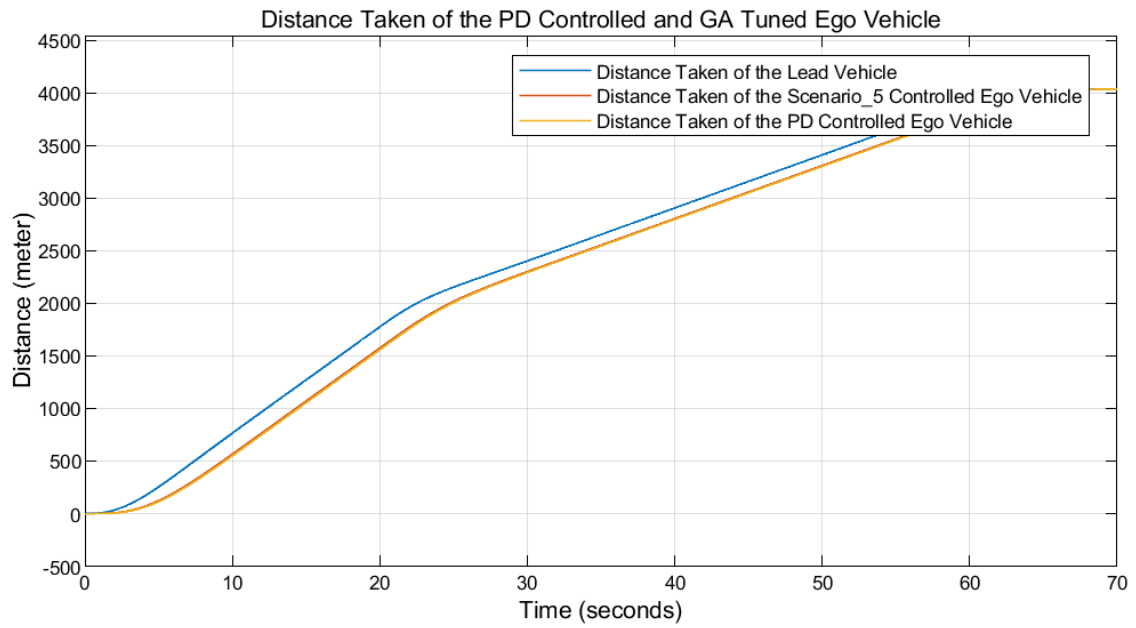


Figure 4.37: Vehicles Distance Comparison of the Two Different Controller

When the distance output shown in Figure 4.37 is examined, two different controllers are cruising very close to each other. There is no violation of ACC norms. However, for clearer data, the distance between vehicles operating with two different controllers should be examined in Figure 4.37.

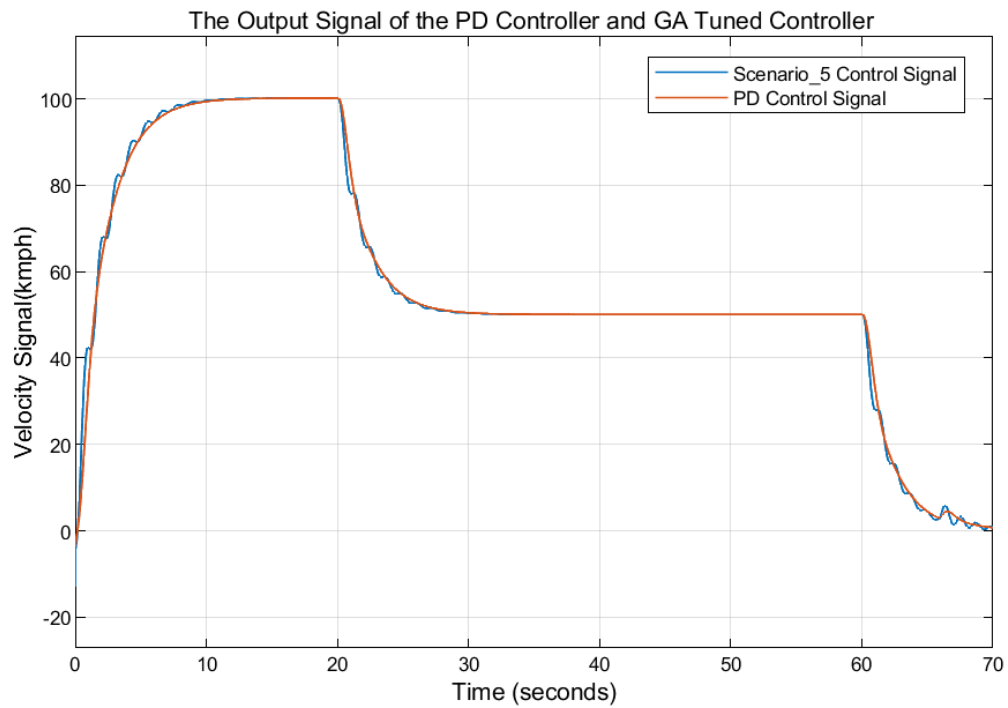


Figure 4.38: Control Signal Comparison of the PD Controller and GA Tuned Controller

When the outputs of control signals are examined, the PD controller designed with the root locus method gives a more stable signal than the controller output tuned with GA. The GA control output, clearly seen in Figure 4.38 oscillates, but when looking at other graphs, the system does not make unstable. In comparison, the aggressive GA control signal may be more difficult to control than the PD controller in some cases.

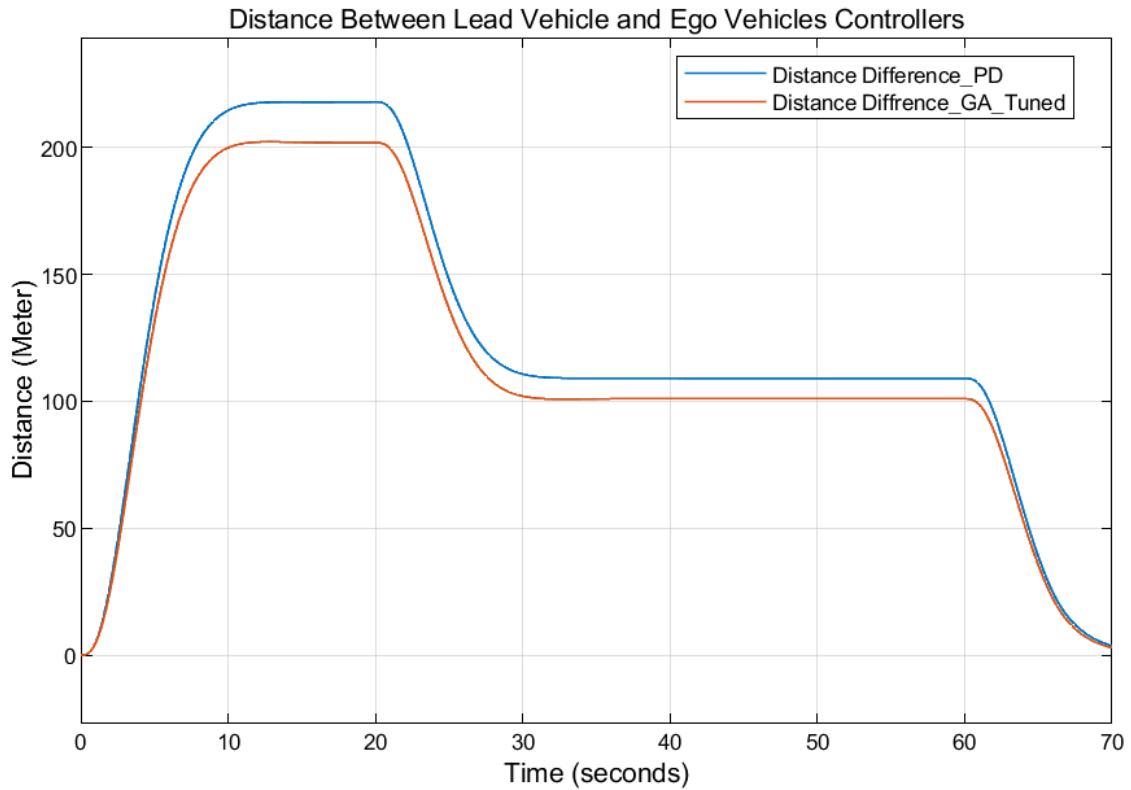


Figure 4.39: Distance Between Lead Vehicle and Ego Vehicle's Controllers

When the distance difference between the two controllers and the leading vehicle is examined in Figure 4.39, the outputs of the controllers in terms of following distance are seen. Clearly, the distance difference seen between 10-20 seconds is 203 meters for the GA controller and 217 meters for the PD controller. The difference between the two scenarios in steady state distance is 14 meters. According to this result, the controller tuned with GA maintains the exact specified following distance.

REALISTIC LIMITS, CONDITIONS AND CONSTRAINS TAKEN INTO CONSIDERATION IN THE DESIGN OF THE PROJECT

Realistic constraints and conditions were taken into consideration while preparing this study. These are as follows:

- The priority in the design of the system is to reduce traffic accidents and reduce the burden on drivers. Considering that the system has been implemented, the use of different communication systems and sensors do not cause any harm to the environment.
- The main purpose of this project is to minimize accidents and protect human life.
- Different controller design approaches have been examined and it can be said that they can be effective in new controller design when the most appropriate results are considered.
- This system, which improves the driving of drivers on long tours, will also benefit different sectors.
- Fast response of the system as standard is also important for Euro NCAP tests. It was taken as standard in the system and it was discussed that there should be a response time of less than 3 seconds. All outputs in the system are under 3 seconds.
- This project, which is open to the improvement of existing systems and the application of different theoretical subjects, can also be used for autonomous driving and convoy problems.
- As a limitation, there was difficulty in finding detailed data in the controller design due to some information being confidential or not shared. We hereby declare that the information and data used are received and used in accordance with ethical values.

CONCLUSION

In this thesis study, a controller design was made for the Adaptive Cruise System. These controllers were tested on the designed non-linear vehicle models and the results were evaluated. In this context, the desired results were obtained from the scenario of vehicles following each other in the Adaptive Cruise System and the desired performance was achieved.

Studies have been carried out on a non-linear model as a simulation model. In the linear model, a linear vehicle model is added to the mathematical model of the system. In the non-linear model, the system was operated by designing a vehicle model close to reality. In this model, gas, brake, gear, engine and transmission subsystems were designed. Vehicle models and mathematical coefficients were chosen to be similar to facilitate the comparison of the results obtained when creating the nonlinear vehicle model.

In this context, for the linear model, the distance and speed results of the other vehicles in the scenario were examined with a reference speed information entered into the leading vehicle. It was observed whether these results met the requirements. In the non-linear vehicle model, the sub-controllers of the following vehicles were also observed and one controller was used for gas and brake. Control coefficients were determined by taking into account the situations where the gas and brake systems operate within the limits of a real vehicle. An optimization method was selected among current and acceptable methods and applied to the controller. Thanks to the convenience provided by the genetic algorithm, manual and tiring prediction application is avoided. On the one hand, a fully theoretical control method was selected and its performance was examined. Predetermined standards were complied with and the design of the system was examined and analyzed. The benefit of the computer environment in estimating methods is also clearly seen.

In the future, studies on artificial intelligence or other optimization algorithms can be carried out to estimate more current controller parameters. Studies can be carried out

on convoy systems and vehicle automation. Studies on the precision and utility of machine learning and older theoretical methods can be highly beneficial.

-
- [1] R. Rajamani, *Vehicle Dynamics and Control*, 2nd Ed., New York: Springer, 2012.
- [2] D. Thomas, S. L. Burton ve B. R. Noack, *Machine Learning Control-Taming Nonlinear Dynamics and Turbulence*, Springer, 2017.
- [3] F. Wegman, «Research to Improve Road Safety,» *SWOV Institute for Road Safety Research the Netherlands*, 2000.
- [4] A. Çavdar, M. Uçar ve İ. Kılıçaslan, «Trafik Kazalarına Sebep Olan Yüksek Hız Kusurlarının Denetimi ve Aktif Güvenlik Sistemler ile Kontrolü,» 2008.
- [5] T. Hacıbekir, «Adaptif Seyir Sistemlerinin Yakıt Yüketimine Etkisinin İncelenmesi,» *İstanbul Teknik Üniversitesi*, 2006.
- [6] «Yıllara Göre Ölümcül ve Ağır Yaralanmalı Kazalar,» [Online]. Available: www.trafik.gov.tr. [Erişildi: 7 Aralık 2023].
- [7] M. Eren ve M. Özdemir, «Doğrusal ve Doğrusal Olmayan Araç Modeli Tasarımı ile Otonom Araçlar İçin Kooperatif Adaptif Seyir Kontrol Sistemi Tasarımı,» YILDIZ TEKNİK ÜNİVERSİTESİ, İSTANBUL, 2020.
- [8] W. Jones, «Keeping Cars from Crashing,» *IEEE Spectrum*, pp. 40-45, 2001.
- [9] Y. Jia ve X. W. Longxiang Guo, «Real-Time Control Systems,» *Transportation Cyber-Physical Systems*, pp. 81-113, 2018.
- [10] D. L. Luu ve C. Lupu, «Dynamics Model and Design for Adaptive Cruise Control Vehicles,» *22nd International Conference on Control Systems and Computer Science IEEE*, 2019.
- [11] M. Short, M. J. Pont ve Q. Huang, «Simulation of Vehicle Longitudinal Dynamics,» University of Leicester, Leicester, 2004.
- [12] Mathworks, «Vehicle with Automatic Transmission Modeling,» [Online]. Available: <https://www.mathworks.com/help/simulink/slref/modeling-an-automatic-transmission-controller.html>.
- [13] «System Identification Toolbox,» [Online]. Available: <https://www.mathworks.com/help/ident/>.

- [14] K. Ogata, Modern Control Engineering, USA: Pearson, 2001.
- [15] Mathworks, «Control System Designer App,» 2024. [Online]. Available: <https://uk.mathworks.com/help/control/ref/controlsystemdesigner-app.html>.
- [16] Mathworks, «Global Optimization,» [Online]. Available: <https://www.mathworks.com/products/global-optimization.html>.
- [17] S. Brunton, «Machine Learning Control, Tuning a PID Controller with Genetic Algorithms,» 2019. [Online]. Available: https://www.youtube.com/watch?v=S5C_z1nVaSg&t=474s.
- [18] mycardoeswhat, «Different ACC Scenarios Animated,» [Online]. Available: www.mycardoeswhat.org.
- [19] T. Bronkhorst, «Hardware Design of a Cooperative Adaptive Cruise Control System Using a Functional Programming Language,» University of Twente, Netherlands, 2014.
- [20] «Waymo,» [Online]. Available: <https://waymo.com/>

RESUME

1. STUDENT PERSONAL INFORMATION

Name SURNAME : Mustafa TURSUN
Birth Place and Date : Stuttgart-Esslingen 16.06.2000
Foreign Language : English
E-mail : mustafatursun2000@hotmail.com
mustafa.tursun@std.yildiz.edu.tr

EDUCATION STATUS

Degree	Field	School/University	Graduation Year
High School	-	Hazım Kulak Anatolian High School	2018

JOB EXPERIENCES

Year	Firm	Duty
2022	Mercedes Benz Türk A.Ş	Engineering Intern

2. STUDENT PERSONAL INFORMATION

Name SURNAME : Anıl Yılmazşamlı
Birth Place and Date : Zonguldak-03.05.1999
Foreign Language : English
E-mail : yilmazsamli@gmail.com

EDUCATION STATUS

Degree	Field	School/University	Graduation Year
High School	-	Zonguldak İ.M.K.B. Anadolu Öğretmen High School	2017

JOB EXPERIENCES

Year	Firm	Duty
2023	Şişli Municipality	Engineering Intern